

EÖTVÖS LÓRÁND UNIVERSITY
CORVINUS UNIVERSITY OF BUDAPEST

PRICING RANGE ACCRUAL PRODUCTS

MSc Thesis

Kristóf Pap

MSc in Actuarial and Financial Mathematics
Faculty of Quantitative Finance

Supervisors:

Dr. Gábor Molnár-Sáska

Eötvös Lóránd University

Department of Probability Theory and Statistics

Dr. Árpád Szilávik



Budapest, 2022

Acknowledgement

I would like to take the opportunity to thank all the people who contributed to the creation of this thesis. I am grateful to my supervisor Dr. Árpád Szilávik for his guidance, and constructive criticism. I would like to thank him for taking the time out of his life to help me write this dissertation. I would also like to thank my other supervisor Gábor Molnár-Sáska, for his help and support.

I am grateful to my classmates for the two years we spent together in this MSc program. Special thanks to Kata for proofreading my thesis.

Finally, I would like to thank my family and friends for always supporting me during my studies.

Contents

1 Introduction	8
2 Product description	10
2.1 What is a range accrual?	10
2.2 Structured notes	12
2.3 Exotic features	12
2.4 Literature overview	13
3 Market models	15
3.1 Range accrual market	15
3.2 Modelling equity dynamics	16
3.2.1 Deterministic volatility models	17
3.2.2 Stochastic volatility models	19
3.3 Sensitivity to stochastic volatility	23
4 Theoretical results	25
4.1 General methodology	25
4.2 Pricing range-accrual notes	27
4.3 Time-dependent Black-Scholes model	29
4.3.1 Calibration	31
4.4 Heston model	32
4.4.1 Calibration	35
4.5 Monte Carlo simulation	37
5 Empirical results	40
5.1 Calibration	40
5.2 Pricing implementation	43
5.3 Sensitivity analysis	44
5.3.1 Product-specific parameters	44
5.3.2 Model parameters	48
6 Summary	52

A Proofs and figures	57
A.1 Proofs	57
A.1.1 Modification of the Black-Scholes formula for the time-dependent case	57
A.1.2 Formula for the European vanilla call option under the Heston model	58
A.1.3 Almost exact simulation of the Heston model	60
A.2 Figures	62
B R code	65

List of Tables

3.1	Specification of different stochastic volatility models	20
5.1	Errors of the Heston model calibration for different weights	41
5.2	Errors of the time-dependent Black-Scholes model calibration	43
5.3	Difference of the numeric integration in the Heston formula compared to	
	accurate prices ($r = 0.01, q = 0.02, S_0 = 100, \theta = 0.25, \kappa = 4, \eta = 1,$	
	$\rho = -0.5$)	44

List of Figures

- 2.1 A multi-period RAN with a maturity of 3 years and 3 coupon periods . . . 11
- 3.1 Implied volatility of European options on the SPX index with 31-day maturity as a function of strike (spot price ≈ 4061). 16
- 3.2 Implied volatilities generated by the Heston model for different maturities ranging from 1 year to 0.4 years. 21
- 4.1 Impact of the volatility of variance parameter (γ in this graph) and the correlation ρ on the IV smile. (Oosterlee & Grzelak, 2019) 35
- 4.2 Impact of mean reversion parameter κ on IV as a function of strike price and time to maturity. (Oosterlee & Grzelak, 2019) 36
- 4.3 Impact of initial variance v_0 and the long run average variance (\bar{v} on this graph) on the IV smile. (Oosterlee & Grzelak, 2019) 36
- 5.1 Implied volatility smiles from the calibrated Heston model (left) and the resulting relative error (right), calibrated with equal weights 42
- 5.2 Relative error from the calibration of the time-dependent Black-Scholes model 43
- 5.3 Effect of the number of observation periods (N) on the price of a range-accrual for the two market models ($c = 10, K^{\text{low}} = 0.9, K^{\text{up}} = 1.1, T = 1$) . 45
- 5.4 Effect of time to maturity on the price of a range-accrual for the two market models ($c = 10, N = 250, K^{\text{low}} = 0.9, K^{\text{up}} = 1.1$) 46
- 5.5 Effect of range parameters on the price of a range accrual for the two market models ($c = 10, N = 250, K^{\text{low}} = 0.9, K^{\text{up}} = 1.1, T = 1$) 47
- 5.6 Price distribution of the time-dependent Black Scholes and Heston models with the calibrated parameters for $T = 0.5$ 47
- 5.7 Effect of the lower barrier value on the price of a range accrual when there is no upper barrier. 48
- 5.8 Effect of the v_0 parameter on the price of a range-accrual and the price of a vanilla call option (The x-axis is the initial volatility, $\sqrt{v_0}$) 49
- 5.9 Effect of the κ parameter on the price of a range accrual and the price of a vanilla call option ($\theta = 0.04$) 50

5.10 Effect of the η parameter on the price of a range accrual and the price of a vanilla call option.	50
A.1 Price distribution of the Heston model for different v_0 parameters	62
A.2 Price distribution of the Heston model for different κ parameters	62
A.3 Price distribution of the Heston model for different η parameters	63
A.4 Effect of the θ , and ρ parameters on the price of a range accrual and the price of a vanilla call option	64

Chapter 1

Introduction

A range accrual is an exotic derivative that accumulates coupon payments when the underlying asset stays within a range. This product is used with many different underlying assets, such as interest rates, stocks, or foreign exchange rates. In the dissertation, I focus on equity markets. My main motivation was that range accruals are usually described in an interest rate market, and I aimed to see what model might be suitable in an equity environment. Therefore, the aim of this thesis is to give a detailed description of range accrual products written on equity underliers including the pricing methodology and the calibration process. Before dwelling on the product and model-specific details, I give a thorough description of the different model families used for equity assets, highlighting the strengths and weaknesses of each model. From the presented models, two are chosen to be the focus of analysis: the time-dependent Black-Scholes model and the Heston model. In my analysis, I show how these two models can be calibrated to market data, and how the range accrual is priced in each model. The given pricing solutions are analytic or semi-analytic, but I also detail the simulation of the Heston model. I do this because pricing via simulation is more robust in the sense that if the paths are already generated, any exotic version of the range accrual can be priced. The thesis is structured as follows.

In Chapter [2](#), I describe the product's payoff, including the single period and multi-period versions. I also list several exotic extensions which can be added to this product. At the end of the chapter, a literature review is given, where the previous works on range accrual pricing are summarised.

In Section [3.1](#), I give an overview of range accrual markets, detailing the underliers which are in use and giving an estimate of the size of the market. Following that, in Section [3.2](#), I describe equity modelling in detail. I list different classes of models which are used for equity derivatives. This section and Section [3.3](#) show the strengths and weaknesses of different models and aim to justify using the Heston model.

Chapter [4](#) begins by introducing some useful concepts used throughout the thesis. Then, a relation between digital options and range accruals is derived. In Sections [4.3](#)

[4.4](#), the two market models are introduced. Analytic formulae for vanilla and digital options are given in both models, as well as the calibration procedure for both. In Section [4.5](#), the simulation of the Heston model is detailed.

In the last chapter, the empirical results are presented. Section [5.1](#) compares the fit of the time-dependent Black-Scholes and Heston models to market data. In section [5.3](#) the sensitivity analysis of Heston model parameters and product parameters is given.

Chapter 2

Product description

In this section, I give a description of the range accrual and an overview of the literature on the product's pricing.

2.1 What is a range accrual?

The range accrual note (RAN) is an exotic derivative that entitles the holder to coupon payments when the underlying asset is in a prespecified range. For every observation period when the underlier is within the range, the product accrues coupons, hence the name. There can be one or more periods, and payments are made after each period. When there is only one coupon determination period, the product pays at maturity, and it is referred to as a single period RAN. Otherwise, it is a multi-period RAN. The payoff of a single period range accrual is the following.

$$\text{payoff} = \text{coupon} \frac{n}{N} \tag{2.1}$$
$$n = \sum_{i=1}^N \mathbb{1}_{\{\text{lower range} < S_i < \text{upper range}\}}$$

Where $\mathbb{1}$ denotes the indicator function, N is the total number of observation periods, and n is the number of periods when the underlying was in the prespecified range. For example, consider a single period range accrual with maturity of one year and a coupon payment of 10. If out of the 252 business days the closing price of the underlying was quoted in the prespecified range 132 times, then the payoff at maturity is $10 \frac{132}{252} = 5.238$. Therefore, in its simplest form, the range accrual pays out the proportion of days the underlier spent in the range multiplied by a constant.

A multi-period range accrual is just a series of single periods RANs, where coupon payments are made at the end of each coupon determination period. The payoff of a

multi-period RAN with d number of coupon determination periods is

$$\text{payoff} = \sum_{j=1}^d \text{coupon}_j \frac{n_j}{N_j} \quad (2.2)$$

$$n_j = \sum_{i=1}^{N_j} \mathbb{1}_{\{\text{lower range}_j < S_i < \text{upper range}_j\}}$$

The payoff is illustrated in Figure 2.1. The product accrues coupons in each period, pays out the coupon at the end of the period, and then starts accumulating coupons again. It can be seen that the lower and upper barriers of the range can change from one coupon determination period to another. It is also possible to only have one barrier, and the other is regarded as infinity. This is especially prevalent in equity markets. The accrued coupon can also change across periods, though it is not common practice. With these features, the range accrual can be tailored to many different market views. The frequency of observations is an implicit parameter of the product. In theory, weekly, monthly, or any custom frequency can be used, however, the market practice is to use daily observations. It can be seen from the payoff that the price of the range accrual does not only depend

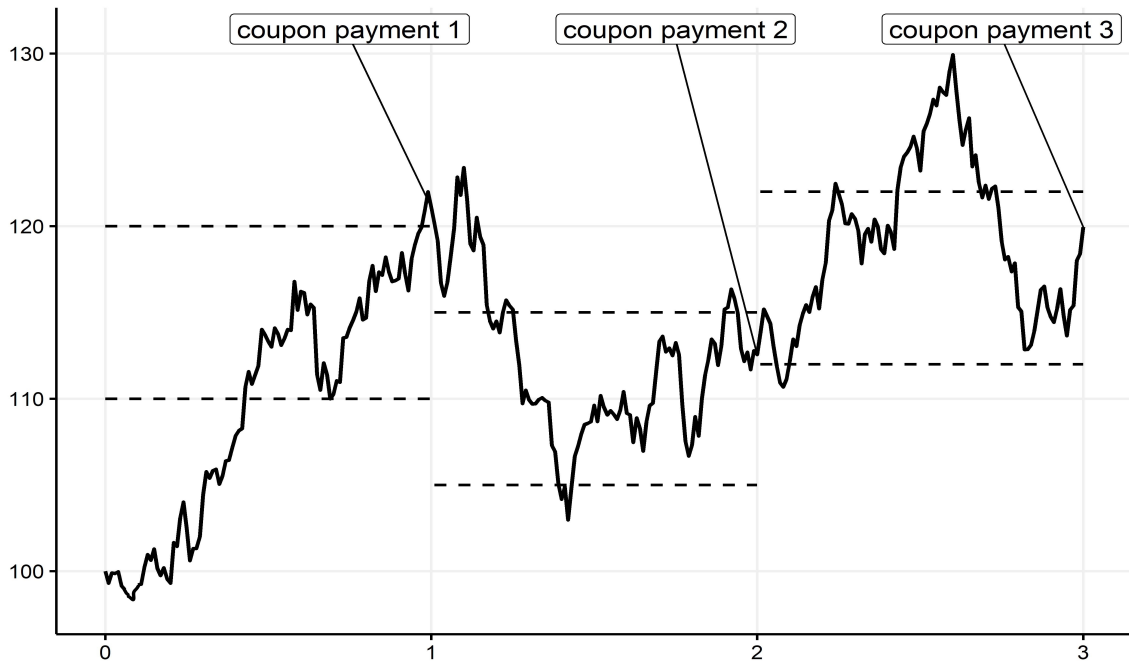


Figure 2.1: A multi-period RAN with a maturity of 3 years and 3 coupon periods

on the final asset price, as in the case of a European option. The whole trajectory of the underlying's price is needed to calculate the payoff. Moreover, range accruals are rarely traded in this basic form, usually, some extra features are added, which further complicate the pricing.

2.2 Structured notes

A range accrual is referred to as a structured derivative or structured product. The term is a wrapper for any pre-packaged financial product which facilitates a custom return structure on an investable asset (Chan et al., 2019). In practice, issuers take a traditional security, such as a bond, and replace the payment with something non-traditional, for example, interest rate swap payments or equity-linked range accrual payments. There are many different variants both for the base security and the payment, even capital protection can be chosen. These products are usually made because standardized contracts do not match the investor's view.

Range accrual notes are usually sold as a structured product, more precisely in the form of a bond, whose payments are the range accrual's coupon payments. This means that the product not only entitles the holder to the coupon payments, but to the payment of the principal amount at maturity as well. The coupons are usually expressed as a percentage of the principal amount. The bond structure is a key feature because it makes this product highly subjected to the credit risk of the issuer.¹ This additional uncertainty is taken into consideration through credit value adjustments, which are usually done separately from the actual pricing. Further information on credit risk can be found in (Hull, 2012), and a detailed description of credit value adjustment is given in (Brigo et al., 2013). I will not detail the credit risk methodology, I will only focus on the pricing of the range accrual coupon payments.

Another problem that arises from the product's structured note nature is that it is not standardized and is usually not exchange-traded. Therefore, there is no easily accessible benchmark price which can be compared to a model result. In an industry environment, it would be theoretically possible to gain access to benchmark data, but it is not feasible for this thesis.

2.3 Exotic features

Despite that the range accrual is already highly customizable, investors had even more specific demands regarding payoffs. This led to the inclusion of additional exotic payoff features on top of the traditional range accrual. These variants became very successful, even so, that it is now rare to see a "vanilla" range accrual without any additional feature. The most common exotic features of range accruals based on (Tan, 2010) and (Chan et al., 2019) are listed.

¹Credit risk is present in any product offering future cash flows, I mean that it is several magnitudes higher if a principal amount is part of the product.

- **Accrual/decruial:** This variant can not only increase the number of days when coupons are accrued but can also decrease it. The decruial range can be different from the accrual range. This feature cheapens the product.
- **Target redemption note (TARN):** The TARN feature repays the note with the principal if the accumulated coupons reach a given level. Meaning that the return is capped by this level, but the investor gets the notional back immediately.
- **Barriers:** Range accruals can be equipped with knock-in and knock-out barriers similarly to vanilla products. This can make the product cheaper at the risk of losing coupon payments.
- **Callable/autocallable:** Similarly to a traditional callable bond, the holder has a short call option on the product, meaning the issuer can decide to buy back the range accrual at a given price. This additional short position cheapens the product. An autocallable note is automatically repaid to the holder if certain conditions are met. It is still a short position but with the autocall feature, the holder is less subjected to the issuer's actions.
- **Basket underlier:** In this variant, the underlier is not a single asset but rather a basket of assets. The range accrual coupon payment is linked to the performance of assets in the basket. It is also possible to combine different asset classes, such as equity, interest rate, and foreign exchange.
- **Floating range accrual:** A floating range accrual does not have a fixed coupon, rather the coupon is determined at the start of each coupon determination period. It can be linked to the same underlying or to some other reference index such as LIBOR.

The list is non-exhaustive, there are many other possibilities to extend the payoff of a range accrual note. I will not go into detail about the pricing methodology of exotic features, because they are too specific for the scope of this thesis.

2.4 Literature overview

A general description of the range accrual product is given in several books focusing on structured derivatives. Two examples mentioned previously are (Chan et al., 2019) and (Tan, 2010). These books also contain the description of exotic features mentioned in Section 2.3.

The first papers dedicated to range accrual pricing were published in the 1990s. It was first proposed by (Turnbull, 1995) that whether the underlying is quoted in the range

or not can be thought of as a binary option with payoff delayed to the end of the coupon determination period. Therefore, the range accrual can be built up from a series of digital options. The author gives a closed-form pricing formula for the range note in the Heath-Jarrow-Morton framework described in (Heath et al., 1992). Following on this idea, (Navatte & Quittard-Pinon, 1999) gives a more simple derivation of the range accrual's price in the same framework. These two articles are considered the first comprehensive descriptions of range accrual pricing. (Nunes, 2004) generalized the pricing from the single factor to the multifactor Gaussian Heath-Jarrow-Morton framework.

Research in the following years focused on finding pricing solutions under more realistic models for the underlying's price evolution, while the overall approach to pricing stayed the same. The most researched asset class is interest rates as range accrual notes are most often used with interest rate underliers. (Chiarella et al., 2014) proposes a pricing method when the underlying follows an affine Wishart process. (Huang, 2011) describes pricing in an affine market model where both the drift and volatility are stochastic and jumps are allowed. (Lin et al., 2017) provides pricing formulae in the LIBOR market model. Regarding the foreign exchange market, (Liao & Hsu, 2009) and (Li et al., 2020) detail the pricing of quanto range accruals.

The area of equity-linked range accruals is not as well-researched, however, there is vast research conducted on equity market models in general. In the following sections, I often use the books of (Gatheral, 2011) and (Oosterlee & Grzelak, 2019) when describing equity modelling. These books also serve as a basis for the comparison of different market models in Section 3.2. The latter book is also referenced in the section where the pricing in the time-dependent Black-Scholes model is discussed. For the pricing of the range accrual note in the Heston model, the works of (Heston, 1993) and (Lazar, 2003) are important, as they show how a vanilla call option and a digital option can be priced under the Heston stochastic volatility model. Regarding the calibration of the Heston model, I use results from (Mrázek & Pospíšil, 2017).

Chapter 3

Market models

In this section, I give an overview of the market of range accruals, showcasing different asset classes. I describe equity dynamics in greater detail, giving an overview of deterministic and stochastic volatility models.

3.1 Range accrual market

Range accruals are not restricted to a single asset class, many different types of underliers can serve as the reference index. Interest rate linked range accruals are very common as it is a principal-protected investment similar to other fixed-income products while having the potential to gain an above-market coupon. The most common underlying interest rates are the 3, 6 and 12-month USD LIBOR, but swap rates or US Treasury rates are also used. Typically, interest rate linked range accruals are long-term investments with maturities of 10 years or more. Equity-linked range accrual notes usually have index underliers, such as the S&P500 and the Dow Jones Industrial Average. In this market, it is common to have only one barrier, typically the lower one, because investors tend to have bullish views on the growth of equity markets. Other underliers include foreign exchange rates, commodity prices, and even inflation rates. The dynamics of these assets are very different, therefore separate modelling is needed for every asset class.

Range accrual notes are over-the-counter products, therefore there is little to no data available about specific trades or the market in general. However, it is known that the overall structured product market is growing. In their article (Faraj & Khaled, [2019](#)) state that the size of the structured product market is about \$7 trillion. This is only about 1% of the total derivatives market, but according to the article, it is bigger than the total ETF or hedge fund markets. It is not known how big of a portion range accrual notes take up from this market, but it does help to put the relative sizes into perspective.

3.2 Modelling equity dynamics

To price equity-linked range accruals, the price evolution of stocks needs to be examined. From 1973, the common practice was to model the stock price as a geometric Brownian motion as in (Black & Scholes, 1973). However, in the late 1980s, especially after the crash of 1987, market prices seemed to violate the Black-Scholes model. The difference between model results and market prices was most apparent in the presence of volatility smiles. The volatility smile is the relationship between the strike price and implied volatility (IV). This can be examined because vanilla options are exchange-traded products and therefore have quoted prices, from which one can calculate the implied volatility associated with that strike and spot price. If the assumptions of the Black-Scholes model were true, a stock's volatility would be constant and thus independent from the spot price and the strike of options written on it. As we can see in Figure 3.1, this is not the case. Implied volatility is lowest for at-the-money or close-to-strike in-the-money options, and as the strike gets further away in either direction, IV increases, giving the smile-like appearance. This shape is not universal, sometimes IV only increases for out-of-the-money options, resulting in a volatility “smirk”. However, the phenomenon that implied volatility changes across strikes and spot prices is observable in every market.

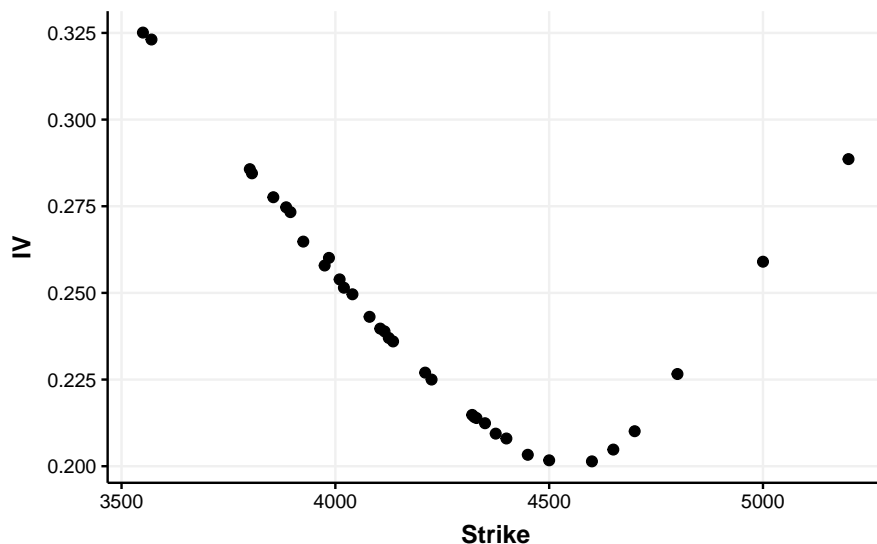


Figure 3.1: Implied volatility of European options on the SPX index with 31-day maturity as a function of strike (spot price ≈ 4061).

Ideal models should not only be able to replicate the volatility smile, but the resulting distributions should replicate the behaviour of returns observed in the market. There are several so-called stylized facts observed in equity markets. Based on (Thompson, 2011) these are the following:

- **Volatility clustering:** The average volatility of returns changes over time. There are highly volatile periods followed by periods with smaller moves
- **Heavy tails:** The empirical distribution of asset returns has heavier tails than the normal distribution. Highly positive or negative returns occur more often than they should if the returns were normally distributed. This is especially true in times of a recession.
- **Leverage effect:** This is the phenomenon that price movements are negatively correlated with volatility. This quantifies the intuition that a bear market is more volatile than a bull one.
- **Long memory and persistence:** These refer to the fact that volatility as a time series has a long memory. External shocks to volatility have a long-lasting effect, rather than disappearing quickly. This manifests in prices, since if volatility has a long memory, then the square of returns has as well. Econometric analysis shows that the higher the frequency of the data, the longer this memory spans.

Models describing equity markets can be loosely categorized into two groups: deterministic and stochastic volatility models[¶]. In the following, I give an overview of the most important models from both of these groups. This section follows the works of (Buraschi & Jackwerth, 2001) and (Vörös, 2018).

3.2.1 Deterministic volatility models

In deterministic models, volatility is regarded as a deterministic function of time and other factors. In this framework, volatility can still depend on stochastic processes, for example, it can be the function of the spot price. There are several attractive features of these types of models. First, they do not introduce a new source of risk, therefore hedging can be achieved with only the underlying asset and the risk-free product. Second, they are usually easy to calibrate, and they can reproduce the volatility smile of equity markets.

- ◇ *Time-dependent Black-Scholes* (Black & Scholes, 1973)

This model is an extension to the original Black-Scholes model in which volatility is a deterministic function of time. The equation governing the stock price is the following.

$$\frac{dS_t}{S_t} = \mu dt + \sigma(t) dW_t$$

The assumption that volatility is a constant parameter was quite restrictive. In this model, volatility can change across time, and thus, it can be calibrated to options

[¶]Some articles treat jump models as a different, third category, here they are described together with SV models.

with different maturities. Moreover, it retains the lognormal asset price distribution of the Black-Scholes model. Therefore, pricing in this model is straightforward, and more importantly, fast. The model's disadvantage is that time dependence is not enough to reproduce the volatility smile, therefore the model can only be calibrated to one strike per maturity. I will compare this model to the Heston model in Section 5.1. I chose the time-dependent Black-Scholes model because I wanted to compare the Heston model to something standard in the industry. As this model has been around for several decades, it is a good point of comparison.

◇ *Local volatility* (Dupire, 1994)

This model is commonly used today, especially in equity markets. Dupire extends the Black-Scholes model by allowing volatility to be dependent on time and the spot price. The stochastic differential equation governing the stock price is given.

$$\frac{dS_t}{S_t} = \mu dt + \sigma(t, S_t) dW_t$$

The term $\sigma(t, S_t)$ is referred to as local volatility. It is a two-dimensional surface that can be calibrated to be consistent with all current European option prices. Local volatility does not represent how volatility actually evolves, it is rather thought of as the expected value of all possible instantaneous volatilities in a stochastic volatility setting (Gatheral, 2011). Therefore, local volatility models are usually used when this average (expected) volatility is sufficient for the pricing of the product.

Dupire gave the equation for calibrating the model to market prices.²

$$\sigma^2(K, T) = 2 \frac{\frac{\partial}{\partial T} C(K, T) + rK \frac{\partial}{\partial K} C(K, T)}{K^2 \frac{\partial^2}{\partial K^2} C(K, T)}$$

Where $C(K, T)$ is the current price of a vanilla call option with T maturity and K strike. This equation gives the unique local volatility from European option prices. This calibration method assumes that there are infinitely many strikes and maturities observed on the options market, which is not a realistic assumption in practice. To circumvent this, numeric methods are used to fit a local volatility surface to discrete data points.

The model is popular because it is relatively fast to calibrate, and it can replicate all the option prices observed in the market. However, the future dynamics of the implied volatility smile are not captured well by this model. Even though it fits the implied volatility surface perfectly in the present, if we calculate the future implied volatilities from the model, the smile flattens, which is unrealistic.

²Dupire originally gave the equation with $r = 0$

◇ *Implied binomial tree* (Rubinstein, 1994)

This method focuses on building a binomial tree for the underlying process, that is consistent with the market prices of options. The structure of the tree is similar to the original Cox-Ross-Rubinstein (CRR) model. (Rubinstein, 1994) gives a method for extracting risk-neutral probabilities from the current volatility smile. Given these probabilities, he shows how to build a unique recombining binomial tree that is consistent with quoted option prices. If the binomial tree is constructed, hedging and pricing can be done similarly to the CRR model. It retains the simplicity of the CRR model while enabling the calibration to market prices.

◇ *Kernel approach* (Aït-Sahalia & Lo, 1998)

The authors use a non-parametric method to calculate risk-neutral densities from quoted option prices. Kernel functions are used to derive an estimator for the risk-neutral density function. This estimator makes it possible to price path-dependent exotic derivatives while being able to reproduce the volatility smile of the market. They argue that a non-parametric method is preferable since it is robust to specification error (model risk) because it is not restricted by parametric assumptions. The drawback of this model is that it is data-intensive to estimate the risk-neutral densities, and in some markets, data is not available in large quantities.

3.2.2 Stochastic volatility models

Stochastic volatility (SV) models introduce a new source of risk by enabling volatility to be stochastic. These models can reproduce the volatility smile, although usually, they can not perfectly replicate it, as some deterministic volatility models do. However, they describe the time evolution of the smile significantly better than deterministic volatility models. Stochastic volatility models also produce more realistic asset price distributions. A disadvantage of SV models is that the introduced source of risk is not directly tradable. This results in an incomplete market, where the risk-neutral martingale measure is not unique.

◇ *Diffusion SV models*

These models describe volatility as a diffusion process, which is separate from the diffusion of the underlying. There are several alternatives for the dynamics of the volatility process. Notable examples of this class include the Heston model (Heston, 1993), the Hull-White model (Hull & White, 1987), the Scott model (Scott, 1987) and the Stein & Stein model (Stein & Stein, 1991). These models share a lot of properties, therefore, not every model is discussed separately.

In the general case, a diffusion SV model takes the form:³

$$\begin{aligned}\frac{dS_t}{S_t} &= \mu(t, S_t)dt + f(v_t)dW_t^1 \\ dv_t &= m(t, v_t)dt + \sigma(t, v_t)dW_t^2 \\ d[W^1, W^2]_t &= \rho dt\end{aligned}$$

In the first equation, it can be seen that v_t is not used directly but rather through the function f . One reason for this is to ensure that volatility stays positive, and this is achieved with some functional transformation. Also, sometimes, instead of volatility, variance is modelled, in that case $f(v_t) = \sqrt{v_t}$. The functions $m(t, v_t)$ and $\sigma(t, v_t)$ specify the dynamics of the v_t process. The driving Wiener processes can be correlated with coefficient ρ . These three functions and the correlation coefficient characterizes diffusion SV models.

model	dv_t	$f(v_t)$
Heston	Cox-Ingersoll-Ross	$\sqrt{v_t}$
Hull-White	geometric Brownian motion	$\sqrt{v_t}$
Scott	Ornstein-Uhlenbeck	e^{v_t}
Stein & Stein	Ornstein-Uhlenbeck	v_t

Table 3.1: Specification of different stochastic volatility models

The defining features of the models mentioned above can be seen in Table [3.1](#). Except for the Hull-White model, all models use a mean-reverting process for v_t . Mean reversion is a desirable feature, as volatility tends to stay in a range instead of growing indefinitely. In the original works of the authors, except for the Heston model, the correlation between driving Wiener processes is assumed to be zero. It is demonstrated in Figure [3.2](#), that diffusion stochastic volatility models are flexible enough to reproduce the volatility smile. The smile flattens for the longer time to maturities, which is in sync with market observations. The empirical properties of asset prices under these models are also favourable. The generated distributions are heavier tailed than the normal distribution and the leverage effect can be achieved by setting $\rho < 0$.

◇ *Jump diffusion SV models*

All the previously mentioned models have continuous trajectories. A straightforward extension is to allow for non-continuous paths by adding jumps to the evolution of the process. One of the first, and probably the most well-known model of this class is Merton's jump-diffusion model (Merton, [1976](#)). In this model, the diffusion

³It is not a fully general case, for example, the correlation coefficient ρ can also be time-dependent.

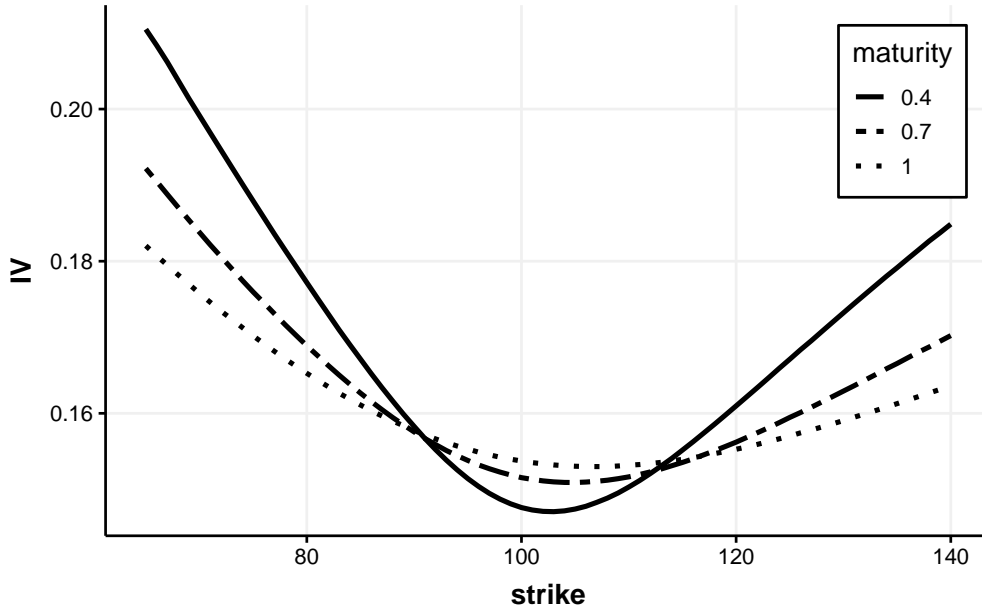


Figure 3.2: Implied volatilities generated by the Heston model for different maturities ranging from 1 year to 0.4 years.

component is similar to a geometric Brownian motion, but a jump component is added. The jump process is a compound Poisson process with lognormal jump size. Jumps are interpreted as external shocks to the market. This model captures the heavy tails of asset returns, and it also has more free parameters than the Black-Scholes model.

The notion that volatility changes stochastically can be incorporated into jump-diffusion models similarly to regular diffusion models. Both the dynamics of the asset price and volatility can contain jumps. A well-known model of this class is the Bates model (Bates, 1996). It describes the asset price with the following stochastic differential equations:

$$\begin{aligned} \frac{dS_t}{S_t} &= (\mu - \lambda \bar{k})dt + \sqrt{v_t}dW_t^1 + kdQ_t \\ dv_t &= \kappa(\theta - v_t)dt + \eta\sqrt{v_t}dW_t^2 \\ d[W^1, W^2]_t &= \rho dt \\ P(dQ_t = 1) &= \lambda dt \end{aligned}$$

Where the term dQ_t is a Poisson process with λ intensity, k is the jump size which is lognormally distributed and \bar{k} is the mean jump size. Essentially, the Bates model adds a compound Poisson process to the Heston model. The trajectories of the asset price contain jumps, but trajectories of variance are still continuous.

This model improves upon the diffusion SV models in several territories. While

diffusion models can reproduce the volatility smile, they generally perform poorly in low maturities. Adding jumps results in a much better fit for these close-to-maturity products. Jumps also give modellers control over how heavy the tail of the asset price distribution should be. This comes at the cost of having a lot of parameters. This not only makes pricing and calibration more complex, but the model can become over parametrized. Some markets are generally less liquid, and the amount of usable data might not be enough to fit these models.

◇ *Pure jump models*

The expected number of jumps in a given interval is finite in jump-diffusion models because the jumps are generated by a Poisson process. Another approach is to use processes that can contain infinitely many jumps on any interval. These models are called pure jump models, as they have no diffusion component. In this framework, log returns are modelled as a pure jump process, such as the Variance Gamma process proposed by (Madan & Seneta, 1990). Then, to get the dynamics of the asset price, some form of exponentiation is used⁴.

These models are generally more flexible than diffusion models. (Barndorff-Nielsen & Shephard, 2001) proposes a method on how to introduce stochastic volatility to pure jump models. This model is referred to as the BNS model, and its dynamics are described by the following equations.

$$\begin{aligned} S_t &= S_0 e^{X_t} \\ dX_t &= (\mu + \beta \sigma_t^2) dt + \sigma_t dW_t + \rho dZ_t \\ d\sigma_t^2 &= -\lambda \sigma_t^2 dt + dZ_t \end{aligned}$$

In this model, there is a Wiener process (W_t) and Lévy subordinator (Z_t) driving the dynamics of log returns, and these processes are independent. The subordinator process Z_t is referred to as background driving Lévy motion, and it adds jumps to both the evolution of variance and returns. If the parameter ρ is negative, a jump⁵ in variance results in a negative jump in returns, capturing the leverage effect. In general, pure jump models capture the empirical properties of asset returns very well, and in some cases, such as the BNS model, semi-analytic formulae can be given for vanilla option prices. Their drawback is that simulating these processes can be more computationally expensive because simulating the background driving Lévy motion involves sampling random numbers from complex distributions.

Naturally, there are many models which were not mentioned. This section aimed to be an overview instead of a complete list. However, there is one additional family

⁴Either applying the exponential function directly to the process or by using the stochastic exponential.

⁵ Z_t is a subordinator, thus it can only have positive jumps

of models which is notable, mixed volatility models. This approach tries to unify the ability of deterministic volatility models to be perfectly calibrated to market prices, with the advantages of stochastic volatility. An example is the stochastic local volatility model described in (Saporito et al., 2019), which extends the local volatility framework to have a stochastic component. This model is popular for products whose price explicitly depends on volatility. Another example is the mixed volatility model (Said, 1999), where variance is given as a product of a deterministic and a stochastic component.

3.3 Sensitivity to stochastic volatility

Stochastic volatility models are more general than deterministic ones in the sense that the latter can be integrated into the former. This is exactly what led to the creation of the previously mentioned mixed volatility models. Because of this, it might be tempting to use a stochastic volatility model in every pricing problem, as the modeller wants to have prices as accurate as possible. However, there are other factors besides accuracy that need to be considered. First, stochastic volatility models are in general more complicated and computationally less tractable. Closed-form solutions rarely exist for exotic derivatives, therefore, one needs to resort to simulation, and SV models are generally more expensive to simulate. Second, the calibration process of stochastic volatility models is generally slow. Fitting SV models usually involves a lengthy numerical calibration, which is not optimal if the goal is to have frequent recalibrations. The industry usually prefers fast methods, because if several thousands of products need to be priced daily, it is not an option to have a slow pricer. Because of this, stochastic volatility models are only used when the product is sensitive to stochastic volatility. Otherwise, the market practice is to use a simpler, deterministic volatility model and account for the stochastic volatility effect in a valuation adjustment. This is sufficient for products that are not, or are weakly sensitive to stochastic volatility.

But what does it mean that a product is sensitive to stochastic volatility? It means that the price of the product strongly depends on the exact path of volatility. In this case, this dependence can not be captured by a valuation adjustment. Products which have volatility as the underlier are highly sensitive to this effect. The two most common examples are volatility and variance swaps.

Another category consists of those products which are not written on volatility itself, but their payoff is implicitly affected by it. To understand this, let us compare a vanilla call option to the same option with an upper knockout barrier. If the barrier level is reached any time during the life of the product, then the option expires worthless, otherwise, it is a traditional call option. In the case of the vanilla call option, the price only depends on the asset price at maturity. Therefore, it does not matter what was the exact trajectory

of volatility, its expected value is enough for pricing the product. However, in the case of the barrier option, one sudden increase in volatility could result in the termination of the trade, and thus, zero payoff. In this case, it is not enough to know the expected value of volatility, it does matter how volatility evolved in time. As mentioned in the previous section, local volatility can be thought of as the expected value of a stochastic volatility model. Therefore, it is sufficient to price those products which are not dependent on the exact path of volatility, but not sufficient if the product is sensitive to this effect. Some products that are sensitive to stochastic volatility include the previously mentioned barrier options, cliquet options, and forward start options.

It will be shown in the later sections how a range accrual can be priced as the sum of a series of delayed digital options. Digital options are not sensitive to stochastic volatility, therefore it is not theoretically required to price a range accrual under a stochastic volatility model. However, I also mentioned before, that range accruals are rarely sold in their vanilla form, usually, some additional features are added, which might require a stochastic volatility model.

Chapter 4

Theoretical results

4.1 General methodology

In this section, a general overview of the pricing methodology is given. The definitions and theorems used throughout the thesis will be described here. The theory of stochastic processes is not discussed here, its main concepts can be found in (Baxter et al., 1996).

Let $(\Omega, \mathcal{F}, \mathcal{F}_t, \mathbb{P})$ be a filtered probability space, where $\{\mathcal{F}_t\}_{t \geq 0}$ is a right-continuous filtration, and \mathbb{P} is a measure on (Ω, \mathcal{F}) , referred to as the statistical or real-world measure. We want to define a market model in this filtered probability space, which consists of a risky asset and a risk-free bank deposit. To define the model, we need the following assumptions.

- The market is arbitrage-free
- There are no transaction fees
- It is allowed to buy any amount of the two assets, short selling included

Assuming a general form of the risky asset, the equations of the model are

$$dB_t = rB_t dt \tag{4.1}$$

$$dS_t = \mu(t, S_t)dt + \sigma(t, S_t)dW_t^{\mathbb{P}} \tag{4.2}$$

The risk-free asset grows at a constant rate r , and the solution to its differential equation is known.

$$B_t = B_0 e^{rt} \tag{4.3}$$

The model is given in terms of measure \mathbb{P} , but for pricing derivatives, the measure needs to be changed to the risk-neutral measure, denoted by \mathbb{Q} . In the risk-neutral measure, the process $\frac{S_t}{B_t}$ is a martingale. The first and second fundamental theorems of asset pricing state the conditions for the existence and uniqueness of the risk-neutral measure. For now,

let us assume that the risk-neutral measure \mathbb{Q} exists and it is unique. Then the dynamics of the risky asset under measure \mathbb{Q} can be determined using the Girsanov theorem \square

Theorem 1 (Girsanov theorem) *If W_t is a Wiener process in measure \mathbb{P} and γ_t is an \mathcal{F} -previsible process with the condition $\mathbb{E}_{\mathbb{P}}[\frac{1}{2} \int_0^T \gamma_t^2 dt] < \infty$, then there exists a measure \mathbb{Q} such that*

- \mathbb{Q} is equivalent to \mathbb{P}
- $\frac{d\mathbb{Q}}{d\mathbb{P}} = \exp\left(-\int_0^T \gamma_t dW_t - \frac{1}{2} \int_0^T \gamma_t^2 dt\right)$
- $\tilde{W}_t = W_t + \int_0^t \gamma_s ds$ is a Brownian motion in measure \mathbb{Q}

The prices of derivatives can be calculated by using the following formula.

Theorem 2 (Risk neutral pricing formula) *Let V_t denote the price of a derivative at time t . The price of any contingent claim at time t , with payoff at maturity V_T is:*

$$\frac{V_t}{B_t} = \mathbb{E}_{\mathbb{Q}} \left[\frac{V_T}{B_T} \mid \mathcal{F}_t \right] \quad (4.4)$$

If B_t evolves as in equation [4.3](#), then

$$V_0 = B_0 \mathbb{E}_{\mathbb{Q}} \left[\frac{V_T}{B_T} \mid \mathcal{F}_0 \right] = e^{-rT} \mathbb{E}_{\mathbb{Q}} [V_T] \quad (4.5)$$

The price of any derivative can be calculated using this formula, but the actual calculation depends heavily on what market model we assume and what is the derivative in question.

Let us assume a model which is less general in terms of the asset price dynamics but contains stochastic volatility.

$$dS_t = \mu_t S_t dt + \sqrt{v_t} S_t dW_t^A \quad (4.6)$$

$$dv_t = \alpha(S_t, v_t, t) dt + \eta \beta(S_t, v_t, t) \sqrt{v_t} dW_t^B \quad (4.7)$$

$$d[W^A, W^B]_t = \rho dt \quad (4.8)$$

This model is generic in the sense that many stochastic volatility models have this form. For example, both the Heston and Hull-White models fit this framework. It is important to note that the appearance of $\sqrt{v_t}$ is just out of practicality, the process is not necessarily a square-root process. For models of this form, a general valuation PDE can be given.

¹Extensions of the Girsanov theorem can be given for a broader set of processes.

Theorem 3 (General valuation equation - (Gatheral, 2011)) *If the market model is the one described in equations 4.6 - 4.8, then the price of any contingent claim $V(t, S, v)$ is governed by the following equation:*

$$\begin{aligned} \frac{\partial V}{\partial t} + \frac{1}{2}vS^2\frac{\partial^2 V}{\partial S^2} + \rho\eta Sv\beta\frac{\partial^2 V}{\partial v\partial S} + \frac{1}{2}\eta^2v\beta^2\frac{\partial^2 V}{\partial v^2} + rS\frac{\partial V}{\partial S} - rV \\ = -(\alpha - \phi\beta\sqrt{v})\frac{\partial V}{\partial v} \end{aligned} \quad (4.9)$$

where $\phi(t, S, v)$ is the market price of volatility risk.

Regarding the market price of volatility risk, (Gatheral, 2011) argues that the risk-neutral drift term can be defined as

$$\alpha' = \alpha - \beta\sqrt{v}\phi \quad (4.10)$$

then the stochastic differential equation of variance becomes

$$dv_t = \alpha'dt + \beta\sqrt{v_t}dW^B \quad (4.11)$$

This way we could get identical results without the need to explicitly estimate the market price of volatility risk. Essentially, by fitting the model to market option prices, we ensure risk-neutral parameters. In the following sections, it is always assumed that the stochastic differential equation of v_t is already in risk-neutral terms.

4.2 Pricing range-accrual notes

As shown in the previous section, the price of a derivative involves calculating the expected value of the discounted payoff in the risk-neutral measure. In this section, I will show how the price of a range-accrual note can be broken down into a series of range digital options with delayed payoffs.

Let $0 < T_1 < \dots < T_N = T$ be the times when the range accrual can accumulate coupons. Consider the payoff of a single period RAN at time T .

$$f_{\text{RAN}}(T) = c\frac{1}{N}\sum_{i=1}^N \mathbb{1}_{\{K^{\text{low}} < S_i < K^{\text{up}}\}}$$

Let $V_{\text{RAN}}(t, T)$ denote the price of a single period RAN, with maturity T , spot asset price S_0 , coupon c , lower barrier K^{low} , and upper barrier K^{up} at time t . The price is calculated by applying the risk-neutral pricing formula to the payoff at time T . The numeraire $B(t)$ is assumed to be the risk-free bank account growing at a constant rate r . The price of the product at $t = 0$ is the following.

$$V_{\text{RAN}}(0, T) = B_0\mathbb{E}_Q \left[\frac{f_{\text{RAN}}(T)}{B_T} \mid \mathcal{F}_0 \right] = \mathbb{E}_Q [e^{-rT} f_{\text{RAN}}(T)]$$

Substituting in the payoff of the product we get

$$= e^{-rT} \frac{c}{N} \mathbb{E}_Q \left[\sum_{i=1}^N \mathbb{1}_{\{K^{\text{low}} < S_i < K^{\text{up}}\}} \right]$$

summation and the expectation can be interchanged

$$= e^{-rT} \frac{c}{N} \sum_{i=1}^N \left(\mathbb{E}_Q \left[\mathbb{1}_{\{K^{\text{low}} < S_i < K^{\text{up}}\}} \right] \right)$$

The indicator function in the expected value can be rewritten as

$$\mathbb{1}_{\{K^{\text{low}} < S_i < K^{\text{up}}\}} = \mathbb{1}_{\{S_i > K^{\text{low}}\}} - \mathbb{1}_{\{S_i > K^{\text{up}}\}}$$

Dividing and multiplying by e^{rt_i} the price of the product becomes

$$V_{\text{RAN}}(0, T) = e^{-rT} \frac{c}{N} \sum_{i=1}^N \left(e^{rt_i} \mathbb{E}_Q \left[e^{-rt_i} \mathbb{1}_{\{S_i > K^{\text{low}}\}} \right] - e^{rt_i} \mathbb{E}_Q \left[e^{-rt_i} \mathbb{1}_{\{S_i > K^{\text{up}}\}} \right] \right)$$

It can be noticed that the two expectations give the price of another derivative, the digital option. This option pays 1 unit if the underlying is above (or below) a prespecified barrier. $\mathbb{1}_{\{S_i > K^{\text{low}}\}}$ is exactly the payoff of a derivative paying 1 unit if $S_i > K^{\text{low}}$, discounting this expression with e^{-rt_i} and taking the expectation gives the price of this product. The same logic applies to the second expectation, it is the price of a digital option that pays 1 unit if $S_i > K^{\text{up}}$. The price of a digital option paying 1 unit at time T if the underlying is above the level K will be denoted as $D(t, T, K)$. The pricing formula can be rewritten as follows:

$$V_{\text{RAN}}(0, T) = e^{-rT} \frac{c}{N} \sum_{i=1}^N \left(e^{rt_i} (D(0, T_i, K^{\text{low}}) - D(0, T_i, K^{\text{up}})) \right) \quad (4.12)$$

The interpretation of this formula is that the RAN can be thought of as a series of range digital options, each paying $\frac{c}{N}$ if the product is in the prespecified range and 0 if it is not. Because this payment is not made immediately, but at the end of the coupon determination period its future value needs to be calculated. This is achieved by multiplying by e^{rt_i} . From this, the price of a multi-period range accrual is the sum of single-period RANs.

$$V_{\text{MRAN}}(0, T) = \sum_{j=1}^D \left[e^{-rT_j} \frac{c_j}{N_j} \sum_{i=1}^{N_j} \left(e^{rt_i} (D(0, T_{i,j}, K_j^{\text{low}}) - D(0, T_{i,j}, K_j^{\text{up}})) \right) \right] \quad (4.13)$$

Where c , K^{low} , K^{up} can all be changing across coupon determination periods, as it was shown in figure [2.1](#), and D is the number of coupon determination periods. The indexing of $T_{i,j}$ corresponds to the coupon accumulation events $0 < T_{1,j} < T_{2,j} < \dots < T_{N_j}$ in period j . Payments are made at the end of each period.

This result enables the pricing of range-accrual notes analytically when the prices of digital options are calculated. This greatly simplifies pricing, as digital options have closed-form or semi-analytic formulas in many market models. The Black-Scholes and Heston models belong in this category, and the formulas for digital options will be given in the following sections.

4.3 Time-dependent Black-Scholes model

In the Black-Scholes model, the asset price is modelled as a geometric Brownian motion

$$dS_t = \mu S_t dt + \sigma S_t dW_t \quad (4.14)$$

with a positive initial value

$$S_0 = s \geq 0$$

The model has two constant parameters: μ controls the drift of the process, and σ is the volatility parameter. The solution to the asset price stochastic differential equation can be found by applying Ito's lemma to the asset price process with the function $f(x) = \ln(x)$.

$$S_t = S_0 \exp \left(\left(\mu - \frac{\sigma^2}{2} \right) t + \sigma W_t \right) \quad (4.15)$$

The Girsanov theorem can directly be applied to change the measure to the risk-neutral one. The Radon-Nikodym derivative defining the risk-free measure is

$$\frac{d\mathbb{Q}}{d\mathbb{P}} = \mathcal{E} \left(\int_0^T \frac{\mu - r}{\sigma} dW_t^{\mathbb{P}} \right) \quad (4.16)$$

where \mathcal{E} denotes the stochastic exponential. The dynamics of the process in the risk-neutral measure is

$$dS_t = r S_t dt + \sigma S_t dW_t^{\mathbb{Q}} \quad (4.17)$$

The measure change only affects the drift, which changed from μ to the risk-free interest rate r . It can easily be seen that the stock price is lognormally distributed, and thus log returns are normally distributed. This is a property that makes pricing less complicated compared to other models. The two derivatives which are important for the purposes of this thesis, the vanilla call and the digital option, both have closed-form prices in the Black-Scholes model. The formula for the vanilla call option enables the calibration of the Black-Scholes model to market prices. The closed-form solution to the digital option means range-accrual prices can be calculated analytically.

Theorem 4 (Black and Scholes, 1973) *If the asset price is a geometric Brownian motion with current spot price S , then the price of a European vanilla call option with*

strike K , maturity T , at time t is

$$V_{call}(t, T, K, S) = SN(d_1) - e^{-r(T-t)}KN(d_2)$$

$$d_1 = \frac{\ln \frac{S}{K} + (r + \frac{\sigma^2}{2})(T-t)}{\sigma\sqrt{T-t}}$$

$$d_2 = d_1 - \sigma\sqrt{T-t}$$

Theorem 5 (Black and Scholes, 1973) *If the asset price is a geometric Brownian motion with current spot price S , then the price of a European digital call option with strike K , maturity T , at time t is*

$$V_{digital}(t, T, K, S) = e^{-r(T-t)}N(d_2)$$

$$d_2 = \frac{\ln \frac{S}{K} + (r - \frac{\sigma^2}{2})(T-t)}{\sigma\sqrt{T-t}}$$

The main problem of the Black-Scholes model is that it fails to reproduce the market prices of options due to the lack of free parameters. The only free parameter of the model is volatility. This one parameter is not enough to fit the model to the market. Therefore, it is common to use some extension of the Black-Scholes model, which enables a better fit to market prices. One common extension is to allow volatility to be a deterministic function of time. This is referred to as the time-dependent (volatility) Black-Scholes model

$$dS_t = \mu S_t dt + \sigma(t) S_t dW_t \quad (4.18)$$

where $\sigma(t)$ is a deterministic function. The asset price is still lognormally distributed.

$$S_t = S_0 \exp \left(\int_0^t \mu - \frac{1}{2} \sigma^2(s) ds + \int_0^t \sigma(s) dW_s \right) \quad (4.19)$$

Because of the lognormal dynamics, the formulas in Theorem 4 and 5 can be extended for the time-dependent case. The standard Black-Scholes formula can be applied with

$$\sigma_* = \sqrt{\frac{1}{T} \int_0^T \sigma^2(t) dt} \quad (4.20)$$

choice for σ . This choice of σ_* equates the first two moments of the distribution of the standard and time-dependent Black-Scholes models, and in the case of the normal distribution, this guarantees equality in distribution. The derivation of σ_* is shown in Appendix A.1.1. Therefore, the previous pricing formulas can be applied with the volatility parameter given in equation 4.20. This only holds for European type payoffs, American type products can not be priced with this method. The two processes will have the same marginal distributions, but nothing guarantees that their transitional distributions will also be the same (Oosterlee & Grzelak, 2019). This result is summarised in the following theorem.

Theorem 6 (Oosterlee and Grzelak, 2019) *If the asset price follows the dynamics of a time-dependent volatility Black-Scholes model with current spot price S and volatility function $\sigma(t)$, then the price of a European vanilla call and digital option with strike K , maturity T , at time t is*

$$\begin{aligned}
 V_{call}(t, T, K, S) &= SN(d_1) - e^{-r(T-t)}KN(d_2) \\
 V_{digital}(t, T, K, S) &= e^{-r(T-t)}N(d_2) \\
 d_1 &= \frac{\ln \frac{S}{K} + (r + \frac{\sigma_*^2}{2})(T-t)}{\sigma_*\sqrt{T-t}} \\
 d_2 &= d_1 - \sigma_*\sqrt{T-t} \\
 \sigma_* &= \sqrt{\frac{1}{T} \int_0^T \sigma^2(t)dt}
 \end{aligned}$$

4.3.1 Calibration

Calibration of the model is an important step in pricing derivatives. This is the process of finding a set of parameter values that provide a good fit to the market which we want to model. The immediate question is to decide what kind of data is used as a reference for the calibration? If the price of the product is quoted on the market, it is straightforward to use that. However, exotic products usually do not have quoted prices, or even if they have, the product might not be liquid enough. In this case, the market practice is to use the prices of vanilla options written on the same underlier. Vanilla option prices are ideal because they are exchange-traded and liquid enough to do frequent recalibrations.

In the time-dependent volatility Black-Scholes model, the spot price S and the risk-free rate r are parameters that are observable on the market. Naturally, the risk-free rate is not directly observable for any arbitrary maturity, but it can be inferred from yield curve data published by federal banks. For the remainder of this thesis, the risk-free rate is assumed to be observed from the US Treasury yield curve.

This leaves $\sigma(t)$ the only object to be calibrated. Because in this model, volatility is only a function of time, there is no way to capture the variation of volatility across strikes. In other words, the model is unable to replicate the volatility smile. Therefore the model can only be calibrated to one strike, which is usually the at-the-money one. The following calibration proposal follows (HochSchule RheinMain, n.d.) Let

$$\sigma_{imp,T_1}, \sigma_{imp,T_2}, \dots, \sigma_{imp,T_m}$$

be the implied volatilities corresponding to the market prices of at-the-money European vanilla call options with maturities T_1, \dots, T_m . To match these implied volatilities in the time-dependent Black-Scholes model, we have to find a function $\sigma(t)$ that satisfies the

equation

$$T_k \sigma_{\text{imp}, T_k}^2 = \int_0^{T_k} \sigma^2(t) dt \quad (4.21)$$

for all of the maturities T_1, \dots, T_m . Rearranging equation [4.21](#), we get

$$T_k \sigma_{\text{imp}, T_k}^2 - T_{k-1} \sigma_{\text{imp}, T_{k-1}}^2 = \int_{T_{k-1}}^{T_k} \sigma^2(t) dt \quad (4.22)$$

We can choose $\sigma(t)$ to be a piecewise constant function, which is equal to σ_k on the (T_{k-1}, T_k) interval. Then we can arrange equation [4.22](#) for σ_k .

$$\sigma_k^2 = \frac{T_k \sigma_{\text{imp}, T_k}^2 - T_{k-1} \sigma_{\text{imp}, T_{k-1}}^2}{T_k - T_{k-1}} \quad (4.23)$$

With this method, we can exactly fit the model to at-the-money options for all of the observed maturities. However, the model will probably not provide a good fit for deep in the money or out-of-the-money strikes. The fit of the time-dependent Black-Scholes model will be compared to the Heston model in the later sections.

4.4 Heston model

The Heston model is described by the following equations

$$dS_t = \mu S_t dt + \sqrt{v_t} S_t dW_t^1 \quad (4.24)$$

$$dv_t = -\kappa(v_t - \theta) dt + \eta \sqrt{v_t} dW_t^2 \quad (4.25)$$

$$d[W^1, W^2]_t = \rho dt \quad (4.26)$$

with initial values

$$S_0 = s \geq 0$$

$$v_0 = v \geq 0$$

Equation [4.24](#) describes the evolution of the asset price, equation [4.25](#) represents the instantaneous variance at time t , and equation [4.26](#) is the covariation of the two driving Wiener processes. The parameters of the Heston model are:

- μ : The drift of the asset price.
- θ : The long-run average variance.
- κ : The rate at which variance reverts to θ .
- η : The volatility of variance.
- ρ : Correlation between the two driving Wiener processes.

- v_0 : Initial value of variance.²

The dynamics of the asset price are similar to the lognormal model, if v_t was deterministic, we would get back the time-dependent Black-Scholes model. The variance process is a Cox-Ingersoll-Ross (CIR) process introduced by (Cox et al., 1985). Using the CIR process for the variance is beneficial for at least two reasons. First, it is mean-reverting, which is desirable because volatility is observed to stay in a range instead of growing indefinitely. Second, it is well known that the CIR process is nonnegative because it can be constructed as the sum of squared of Ornstein-Uhlenbeck processes. Moreover, if the initial value of the process is not zero and the Feller condition is satisfied,

$$2\kappa\theta > \eta^2 \quad (4.27)$$

the process will never reach zero. This is favourable because no functional transformation is needed to ensure positivity in the Heston model. However, when fitted to real market data, the Feller condition often does not hold.

To calculate option prices in the Heston model, a risk-neutral measure is needed. As described in (Márkus, 2017), an extension of the Girsanov theorem can be used to determine the risk-neutral measure.

$$\frac{d\mathbb{Q}}{d\mathbb{P}} = \mathcal{E} \left(\int_0^T \frac{r - \mu}{\sqrt{v_t}} dW_t^{1,\mathbb{P}} \right) \quad (4.28)$$

Under the \mathbb{Q} , measure the process $W_t^{1,\mathbb{Q}} = W_t^{1,\mathbb{P}} + \frac{r - \mu}{\sqrt{v_t}}$ will be a Wiener process and the risk-neutral dynamics of the asset price will be

$$dS_t = rS_t dt + \sqrt{v_t} S_t dW_t^{1,\mathbb{Q}} \quad (4.29)$$

Thus, the measure change only affects the drift μ , and similarly to the Black-Scholes model, the growth rate of the asset price is the constant risk-free interest rate.

The last step for calculating option prices in the model is to determine the partial differential equation which gives the price of any contingent claim in the model. This can be easily achieved by substituting into the general valuation equation in Theorem 3. Let $V(t, S, v)$ be the price of a derivative at time t , with spot asset price S , and instantaneous variance v . Then, the partial differential equation governing the price of the derivative is

$$\frac{\partial V}{\partial t} + \frac{1}{2}vS^2 \frac{\partial^2 V}{\partial S^2} + \rho\eta Sv \frac{\partial^2 V}{\partial S \partial v} + \frac{1}{2}\eta^2 v \frac{\partial^2 V}{\partial v^2} + rS \frac{\partial V}{\partial S} - \kappa(v - \theta) \frac{\partial V}{\partial v} - rV = 0 \quad (4.30)$$

with an appropriate boundary condition.

One of the main advantages of the Heston model is that there exists a formula that satisfies this equation for the European vanilla call option. This enables the fast and efficient calibration of the model. This result is given in the following theorem

²It is regarded as a parameter because it cannot be observed in the market, therefore it is usually fitted during the calibration process.

Theorem 7 (Heston, 1993) *If the asset price follows the dynamics of the Heston model described in equations 4.24-4.26 with current spot price S , then the price of a European vanilla call option with strike K , and maturity T at time t is*

$$V_{call}(t, T, K, S, v) = SP_0 - e^{-r(T-t)}KP_1$$

$$P_j(x, v, \tau) = \frac{1}{2} + \frac{1}{\pi} \int_0^\infty \operatorname{Re} \left\{ \frac{\exp\{C_j(u, \tau)\theta + D_j(u, \tau)v + iux\}}{iu} \right\} du$$

For $j = 0, 1$, $x = F_{t,T}/K$ and $\tau = T - t$

$$D(u, \tau) = r_- \frac{1 - e^{-d\tau}}{1 - ge^{-d\tau}}$$

$$C(u, \tau) = \theta \left\{ r_\tau - \frac{2}{\eta^2} \log \left(\frac{1 - e^{-d\tau}}{1 - g} \right) \right\}$$

$$\alpha = -\frac{u^2}{2} - \frac{i u}{2} + i j u, \quad \beta = \theta - \rho \eta j - \rho \eta i u, \quad \gamma = \frac{\eta^2}{2}$$

$$r_\pm = \frac{\beta \pm \sqrt{\beta^2 - 4\alpha\gamma}}{2\gamma} = \frac{\beta \pm d}{\eta^2}, \quad g = \frac{r_-}{r_+}$$

This formula can be evaluated with numerical integration to a sufficient degree of accuracy. The accuracy of this method will be tested in Section 5.2

Determining the price of a vanilla call option is important because of the calibration process. But for pricing range accruals, digital option prices should be calculated. A digital option pays 1 unit if the underlying is above a prespecified barrier and zero otherwise.

$$V_{digital}(T, S, v) = \mathbb{1}_{\{S_T > K\}} \tag{4.31}$$

If we take the expectation in the risk-neutral measure, the price of this option is the probability that the option will expire in the money multiplied by a discount factor. This is exactly the P_1 pseudo-probability calculated previously. Therefore, the price of a digital option can be directly calculated using the previous results. A formal proof of the digital price can be found in (Lazar, 2003)

Theorem 8 (Lazar, 2003) *If the asset price follows the dynamics of the Heston model described in equations 4.24-4.26 with current spot price S then the price of a digital option with strike K , and maturity T at time t is*

$$V_{digital}(t, T, K, S, v) = e^{-r(T-t)}P_1$$

Where P_1 is calculated as in Theorem 7.

4.4.1 Calibration

The Heston model has seven parameters, out of which two are directly observable on the market. These two are the spot asset price S_0 , and the risk-free rate r . As previously mentioned, the risk-free rate is inferred from US Treasury yield curve data. The parameters that are not observable and need to be calibrated are $\Pi = (\rho, v_0, \theta, \kappa, \eta)$. In the following, it is shown how the implied volatilities of vanilla options are affected by these parameters. In each case, the value of one parameter is varied, while the others are held fixed.

The effect of parameters η and ρ is illustrated in Figure 4.1. On the left graph, it can be seen that the lower the volatility of variance, the flatter the smile. Thus, the volatility of variance parameter controls the curvature of the smile. Higher values of the correlation parameter ρ give a regular smile, and lower values give a more skewed IV smile. The latter is more common in equity markets. The parameter κ controls the speed of mean reversion of the variance process. In the left graph of Figure 4.2, it can be seen that as a function of strike, κ has the effect of an almost parallel shift. As a function of time to maturity, greater κ values contribute to a more concave IV shape. This is because as κ increases, variance converges faster to its mean. The remaining two parameters have similar effects, as seen in Figure 4.3. The effect of the long-run average variance parameter θ across strikes is a parallel shift, and the effect of initial variance v_0 is an almost parallel shift across time to maturities.

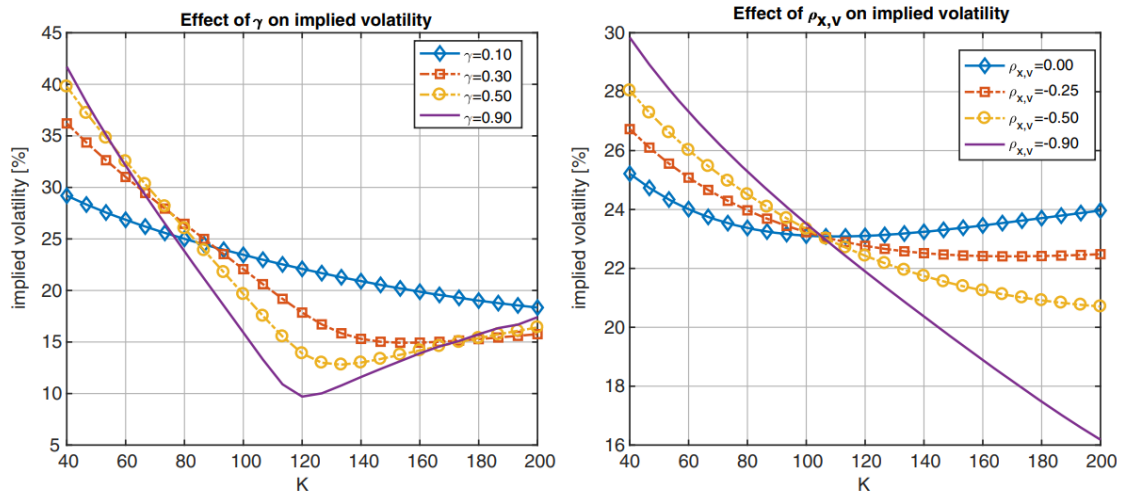


Figure 4.1: Impact of the volatility of variance parameter (γ in this graph) and the correlation ρ on the IV smile. (Oosterlee & Grzelak, 2019)

The reference data for calibration consists of vanilla option prices written on the same underlier as the product we want to price. This data is publicly available for numerous stocks and indices, for example, on yahoo finance. The Heston model does not have

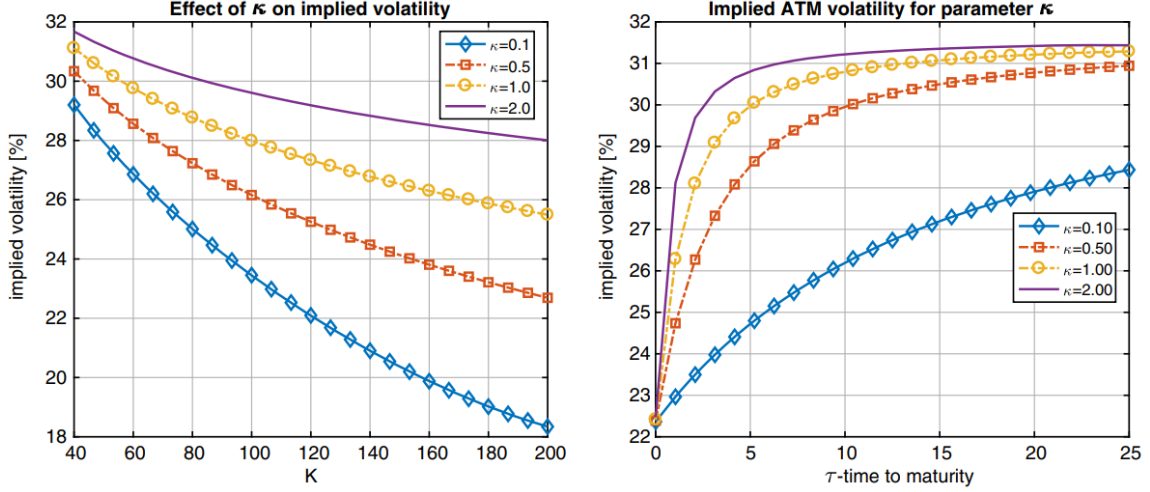


Figure 4.2: Impact of mean reversion parameter κ on IV as a function of strike price and time to maturity. (Oosterlee & Grzelak, 2019)

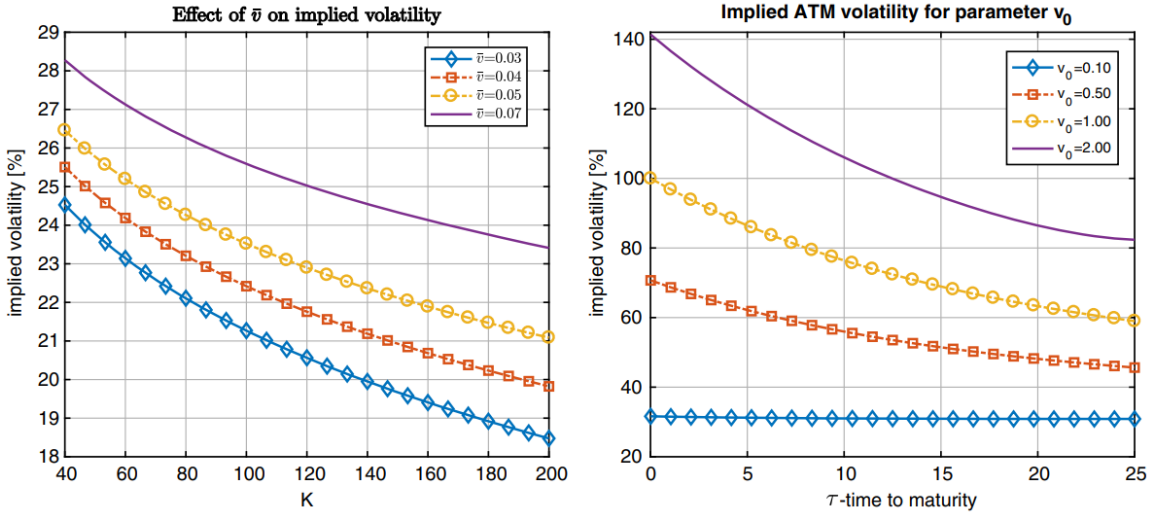


Figure 4.3: Impact of initial variance v_0 and the long run average variance (\bar{v} on this graph) on the IV smile. (Oosterlee & Grzelak, 2019)

enough free parameters to exactly fit market implied volatilities across all strikes and maturities. Therefore, the calibration process becomes an optimization problem. The aim is to minimize the error between model prices and market prices. Measuring this error is a modelling question. There are several alternatives, the most common being the sum of squared differences. With this error metric, the task results in a nonlinear least squares optimization problem.

$$\min_{\Pi} \sum_i \sum_j w_{i,j} (V^*(t_0, S_0, K_i, T_j) - V(t_0, S_0, K_i, T_j, \Pi))^2 \quad (4.32)$$

Where $V^*(t_0, S_0, K_i, T_j)$ is the market price at time t_0 and spot asset price S_0 for a vanilla

call option with strike K_i and maturity T_j , and $V(t_0, S_0, K_i, T_j, \Pi)$ is the Heston price for the same call option with parameter set Π . $w_{i,j}$ is the weight associated with that particular strike and maturity. The weights can be equal, in that case, $w_{i,j} = 1$. If the weighting is not constant, more liquid options are usually given bigger weights, as it is more important for the model to match liquid option prices than illiquid ones. Liquidity is usually measured with the size of the bid-ask spread. Some alternatives for the weights are listed below, with spread indicating the bid-ask spread associated with the option for a given maturity and strike.

$$A = \frac{1}{|\text{spread}|} \quad (4.33)$$

$$B = \frac{1}{(\text{spread})^2} \quad (4.34)$$

$$C = \frac{1}{\sqrt{\text{spread}}} \quad (4.35)$$

The optimization problem can also be formulated in terms of implied volatilities

$$\min_{\Pi} \sum_i \sum_j w_{i,j} (\sigma^*(t_0, S_0, K_i, T_j) - \sigma(t_0, S_0, K_i, T_j, \Pi))^2 \quad (4.36)$$

In this case, $\sigma^*(t_0, S_0, K_i, T_j)$ is the implied volatility associated with the market price of a vanilla call option, and $\sigma(t_0, S_0, K_i, T_j, \Pi)$ is Heston model-implied volatility.

The problem with this optimization is that the function described in equations [4.32](#) and [4.36](#) is not convex, and it is also not of any recognizable structure (Mrázek & Pospíšil, [2017](#)). Moreover, the parameters of the Heston model are not independent in the sense that the effect of different parameters on the implied volatility smile can be similar. Because of this, several sets of parameters might provide a good fit, resulting in numerous local minima to the error function. It is also a constrained optimization problem as $\rho \in [-1, 1]$ and $\kappa, v_0, \eta, \theta \geq 0$.

There are several numerical methods to solve such an optimization problem. In this thesis, the limited-memory BFGS method is used³. This algorithm uses an estimate of the inverse of the Hessian matrix to search for a local minimum. The algorithm is implemented in the R programming language by default. It allows for constraints on the optimized variables, and given a set of initial values, it converges in a reasonable time.

4.5 Monte Carlo simulation

In order to price derivatives with the Monte Carlo method, sample paths of the Heston process need to be generated. It is particularly challenging to generate paths from the

³A detailed description of the limited memory Broyden–Fletcher–Goldfarb–Shanno algorithm can be found in (Byrd et al., [1995](#))

CIR process. In the following, I present several alternatives on how to simulate values from the dynamics described in equations [4.24](#), [4.25](#), and [4.26](#).

Euler method

The Euler (or Euler-Maruyama) method is a well-known discretization technique for SDEs. It is described in detail in (Márkus, [2017](#)). The Euler discretization of the variance process with equal timesteps of Δt is

$$v_{i+1} = v_i + \kappa(\theta - v_i)\Delta t + \eta\sqrt{v_i}\sqrt{\Delta t}Z_1 \quad (4.37)$$

where $Z_1 \sim N(0, 1)$. As stated previously, if the Feller condition (eq. [4.27](#)) holds, the trajectories of the process are nonnegative. However, this statement is not true if the process is discretized, the discrete process can become negative with a positive probability (Mrázek & Pospíšil, [2017](#)). Moreover, we also need to be able to simulate sample paths if the parameters violate the Feller condition. The two standard ways of solving the negativity problem are the absorbing method⁴: if $v < 0$ then $v = 0$, or the reflecting method: if $v < 0$ then $v = -v$ (Gatheral, [2011](#)). If $\Delta t \rightarrow 0$, the estimation is bias-free regardless of the chosen method.

The Euler discretization for the asset price is

$$S_{i+1} = S_i + \mu S_i \Delta t + \sqrt{v_i} S_i \sqrt{\Delta t} Z_2$$

where Z_2 is also standard normal and $\text{corr}(Z_1, Z_2) = \rho$. Usually, not the asset price, but the log returns ($X_i = \log(S_i/S_0)$) are discretized, because this way there is no higher-order correction needed for the Euler discretization. The discretization for the log returns is

$$X_{i+1} = X_i + \left(\mu - \frac{1}{2}v_i \right) \Delta t + \sqrt{v_i} \sqrt{\Delta t} Z_2 \quad (4.38)$$

From this $S_{i+1} = S_0 e^{X_{i+1}}$. Therefore exponentials need to be taken for each timestep, however, with modern computational power, this does not slow down the simulation.

Milstein method

The Milstein scheme is similar to the Euler, but it uses a higher-order form of the Ito-Taylor expansion (Gatheral, [2011](#)). The Milstein discretization for the variance process with the same notation as before is

$$v_{i+1} = v_i + \kappa(\theta - v_i)\Delta t + \eta\sqrt{v_i}\sqrt{\Delta t}Z_1 + \frac{\eta^2}{4}\Delta t(Z_1^2 - 1) \quad (4.39)$$

It is the same as the Euler scheme, except the extra correction term $\frac{\eta^2}{4}\Delta t(Z_1^2 - 1)$. Gatheral points out that by using the Milstein method, the occurrences of negative variances are

⁴Sometimes referred to as full-truncation method.

substantially reduced, even when parameters do not satisfy the Feller condition. However, negative values can still occur with nonzero probability, thus, either the reflection or absorbing methods should be used to counteract this. As stated previously, the Milstein discretization of log returns does not require any higher-order corrections, therefore in the Milstein scheme, it can still be simulated as in equation [4.38](#).

Almost exact simulation

The Euler and Milstein methods can be used to simulate any stochastic differential equation, even when the solution is not known explicitly. However, when the exact distribution of the process at time t is known, random numbers can be sampled from the distribution, eliminating the problems which arise from the discretization of the time grid. In the case of the CIR process, the exact distribution is known to be the noncentral chi-squared distribution (Cox et al., [1985](#)). Conditioning on the previous state of the process $v(s)$, $s < t$, the distribution of the CIR process at time t is

$$v(t)|v(s) \sim c(t, s)\chi^2(\delta, \lambda(t, s)) \quad (4.40)$$

where

$$c(t, s) = \frac{\eta^2}{4\kappa} (1 - e^{-\kappa(t-s)}), \quad \delta = \frac{4\kappa\theta}{\eta^2}, \quad \lambda(t, s) = \frac{4\kappa e^{-\kappa(t-s)}}{\eta^2(1 - e^{-\kappa(t-s)})}v(s) \quad (4.41)$$

In this notation, c is a constant multiplier and $\chi^2(\delta, \lambda)$ denotes the noncentral chi-squared distribution with δ degrees of freedom and noncentrality parameter λ . If the previous value of variance is known, then the current variance can be sampled directly from the given distribution. It can also be noted, that the previous variance value $v(s)$ is only influencing the next value through the noncentrality parameter. The almost exact approximation of the Heston process with timestep Δt is the following.

$$X_{i+1} = X_i + \left(\mu - \frac{1}{2}v_i \right) \Delta t + \frac{\rho}{\eta} (v_{i+1} - v_i - \kappa(\theta - v_i)\Delta t) + \sqrt{1 - \rho^2} \sqrt{v_i} Z \quad (4.42)$$

$$v_{i+1} = c(t_{i+1}, t_i)\chi^2(\delta, \lambda(t_{i+1}, t_i)) \quad (4.43)$$

where c , δ , and λ are parameters defined in equation [4.41](#), and $Z \sim N(0, 1)$. A detailed derivation of this result is given in Appendix [A.1.3](#). This simulation method is referred to as almost exact because the sampling of the variance process is exact but for the returns process, Euler approximations were used. Using this method, the problem of negative variance never arises because the exact distribution of the CIR process is used. Another advantage, as argued by (Oosterlee & Grzelak, [2019](#)), is that it requires fewer time steps than the Euler and Milstein methods to give accurate results for derivatives prices. The only downside of this method is that it requires random number sampling from the noncentral chi-squared distribution, which is computationally more intensive than sampling from the normal distribution. However, most modern programming languages have libraries that are optimized for this task.

Chapter 5

Empirical results

In the previous chapter, it was shown how a range accrual product can be priced under the time-dependent Black-Scholes and Heston models. The calibration processes of these models were also discussed. These results are implemented in the R programming language and will be presented in this section. The code used for the implementation is available in Appendix [B](#).

5.1 Calibration

To calibrate the models, market data was obtained from the yahooFinance stock and option monitoring website. I used options written on the S&P500 equity index, as it is a common underlier for equity products. The models are calibrated to 3 maturities: 0.5, 1 and 1.65 years, each having 50-80 strikes. The risk-free rate is assumed to be the one year US Treasury zero-coupon rate, which at the time of the calibration was $r = 1.338\%$. The spot price of the index at the time was 4478.28. To evaluate the resulting model fit, three different error measures are used.

$$\text{maximum absolute relative error: } \text{MARE}(\Pi) = \max_i \frac{|\sigma_i^\Pi - \sigma_i^*|}{\sigma_i^*} \quad (5.1)$$

$$\text{average absolute relative error: } \text{AARE}(\Pi) = \frac{1}{n} \sum_{i=1}^n \frac{|\sigma_i^\Pi - \sigma_i^*|}{\sigma_i^*} \quad (5.2)$$

$$\text{root-mean-square error: } \text{RMSE}(\Pi) = \frac{1}{n} \sqrt{\sum_{i=1}^n (\sigma_i^\Pi - \sigma_i^*)^2} \quad (5.3)$$

Where σ^* denotes the implied volatility on the market and σ^Π indicates the model implied volatility associated with the parameter set Π . I will calibrate all models to implied volatilities instead of option prices. If I were to calibrate to option prices directly, some normalization would be needed, because in-the-money option prices are fairly larger than out-of-the-money ones, and the calibration would be overfitted to the in-the-money side. Using implied volatilities serves as a natural normalization.

I calibrated the Heston model with the numerical optimization method described in Section 4.4.1. I used four different weightings, described in equations 4.33-4.35, and an additional equal weighting. None of the weightings resulted in a significantly different set of parameters than the others. The errors of the fitted models are shown in Table 5.1. The error measures confirm that there is no single superior weighting, they all have similar performance.

weights	RMSE	AARE	MARE
A	0.00551	0.01832	0.1429
B	0.00575	0.02201	0.1042
C	0.00559	0.01833	0.1453
equal	0.00549	0.02032	0.1319

Table 5.1: Errors of the Heston model calibration for different weights

To have a better view of how good the fit is, I plotted the model-implied volatilities from the equal weighting calibration against the market data and the resulting error in Figure 5.1. The volatility smile is flatter for the longer maturities of 1 and 1.65 years, resulting in a more smirk-like shape. This is in line with the empirical finding that the smile tends to flatten on longer maturities. The fit is also better for these longer maturities. On the shorter 0.5 years maturity, the volatility smile is more pronounced, and the Heston model has trouble fitting the smile, especially in the deep in-the-money part. This is in agreement with other studies, where researchers found that the model has a tendency to misprice short-term options (Shu & Zhang, 2004). This is not a unique problem of the Heston model, in fact, most pure diffusion models tend to misprice short-term options. One solution is to incorporate jumps in the model to capture the short-term variation in option prices. These models, particularly infinite activity jump models were shown to have a better fit for short-term options (Mijatović & Tankov, 2016). Taking this into consideration, the fit of the Heston model is acceptable.

The time-dependent Black-Scholes model has no parameters to fit the implied volatility smile in the strike dimension. Therefore, the model is calibrated to the at-the-money implied volatility for each maturity as in Section 4.3.1. This results in a flat volatility smile for each maturity, where the model exactly matches the at-the-money volatility but fails to replicate the in-the-money or out-of-the-money volatilities. This can be observed in Figure 5.2, as the error is zero for the at-the-money strike, and grows linearly in both directions, reaching 40% on the sides. The error measures of the fit, as seen in Table 5.2, are a magnitude higher than the Heston's.

It can be concluded that the Heston model provides a much better fit to market data than the time-dependent Black-Scholes model. It can incorporate the variation of option prices in the strike dimension, albeit not perfectly. If the goal is to fit the market

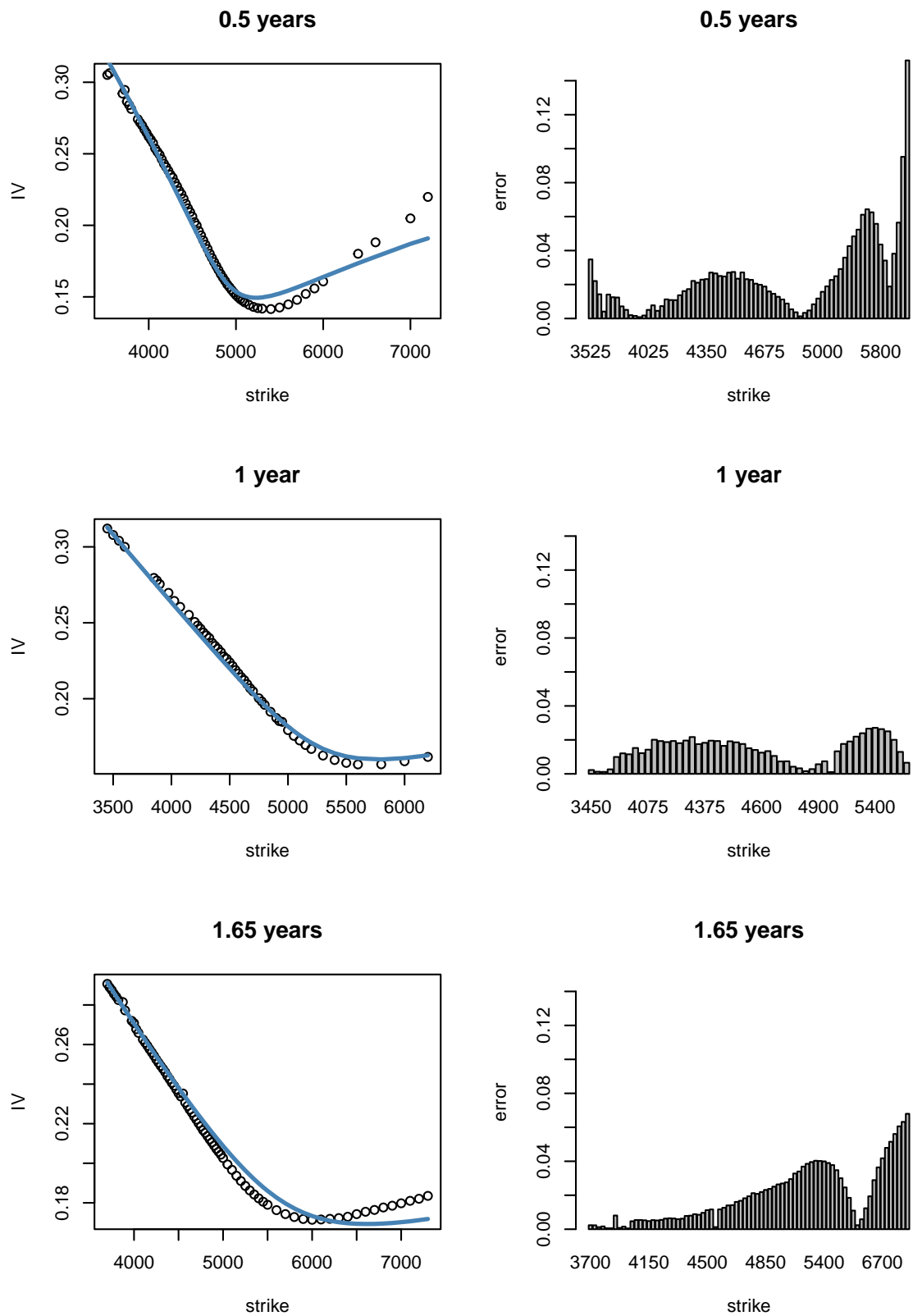


Figure 5.1: Implied volatility smiles from the calibrated Heston model (left) and the resulting relative error (right), calibrated with equal weights

RMSE	AARE	MARE
0.04505	0.19302	0.47873

Table 5.2: Errors of the time-dependent Black-Scholes model calibration

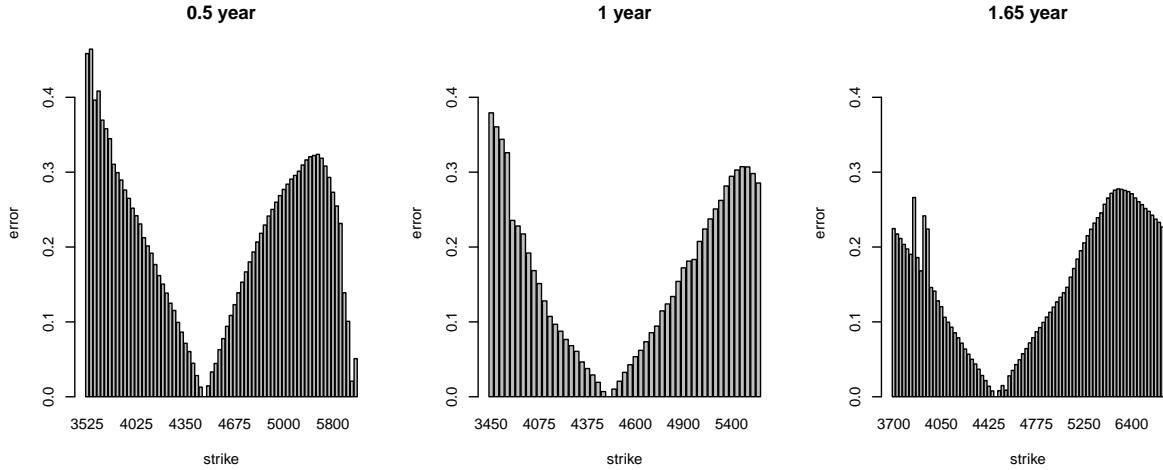


Figure 5.2: Relative error from the calibration of the time-dependent Black-Scholes model

prices perfectly in a stochastic volatility model, the previously mentioned stochastic local volatility model might be used.

5.2 Pricing implementation

In Section [4.2](#), it was shown that a range accrual could be priced as a series of range digital options with delayed payments (eq. [4.12](#), [4.13](#)). The formula for digital options in the Heston model was also given, however that formula involved calculating an integral of a function that has no closed-form antiderivative. There are several alternatives to calculate the integral in theorem [8](#), here I will use a modified version of the *callHestoncf* function implemented in the R package called NMOF. This method uses R's built-in numerical integration to evaluate the integral. This method yields low errors, despite the complexity of the function and the interval being infinite. To demonstrate this, I compared call prices from the R implementation to high accuracy option prices. The reference prices were calculated by (Lewis, [2019](#))¹ and they are accurate up to 15-20 digits. There are two cases, one with longer maturity ($T = 1$) and greater starting variance ($v_0 = 0.04$), and one with an extremely short maturity ($T = 0.01$) and lower initial variance ($v_0 = 0.01$). In both cases, the R implementation is accurate at least up to the first four digits, and in the less extreme one year time to maturity, it is accurate up to 6-10 digits. Based on this, I conclude that the R implementation is accurate enough for the following pricing

¹The dataset of reference prices can be found on the link in references.

demonstrations.

strikes	T = 1, $v_0 = 0.04$	strikes	T = 0.01, $v_0 = 0.01$
80	0.0000000015	90	-0.0000444993
90	-0.0000002814	95	0.0000038739
100	0.0000000000	100	0.0000000050
110	0.0000000000	105	-0.0000003414
120	-0.0000000099	110	0.0000142476

Table 5.3: Difference of the numeric integration in the Heston formula compared to accurate prices ($r = 0.01$, $q = 0.02$, $S_0 = 100$, $\theta = 0.25$, $\kappa = 4$, $\eta = 1$, $\rho = -0.5$)

5.3 Sensitivity analysis

In this section, the pricing results of the two different models will be presented along with a sensitivity analysis of parameters. First, I analyze the sensitivity to product parameters, then the sensitivity to model parameters.

5.3.1 Product-specific parameters

Let us examine the effect of product-specific parameters to the price of a single period range accrual. The previously calibrated parameters will be used, which are

$$r = 0.01338, S_0 = 4478.28, v_0 = 0.0399, \theta = 0.1415, \kappa = 1.0038, \eta = 1.0030, \rho = -0.7726$$

for the Heston case, and

$$r = 0.01338, \sigma(t) = \begin{cases} 0.2092 & 0 \leq t < 0.5 \\ 0.2423 & 0.5 \leq t < 1 \\ 0.2534 & 1 \leq t < 1.65 \end{cases}$$

for the time-dependent Black-Scholes case. The range accrual has five product-specific parameters, which will be examined in this order.

- c : coupon payment
- N : number of observation periods
- T : maturity
- K^{low} : lower barrier of the coupon payment range
- K^{up} : upper barrier of the coupon payment range

The effect of coupon payment is just a multiplier on the price of the range accrual, therefore, the first parameter to be analyzed is the number of observation periods. Changing this parameter does not affect the maximum coupon payment during the life of the product, as each payment is $\frac{c}{N}$. What it affects is the number of times it is checked whether the underlying is quoted in the range. The effect of this parameter can be seen in Figure 5.3. As the number of observation periods increases, so does the price of the product, but at around $N = 100$, it converges and a further increase in N has little to no effect on the price. This is the effect of the discrete monitoring converging to the continuous case. It can also be noted that the price is higher in the case of the Heston model than in the time-dependent Black-Scholes case. This is caused by the shape of the density functions, as the Heston is more concentrated to the $(0.9, 1.1)$ interval where the product pays coupons (Figure 5.6).

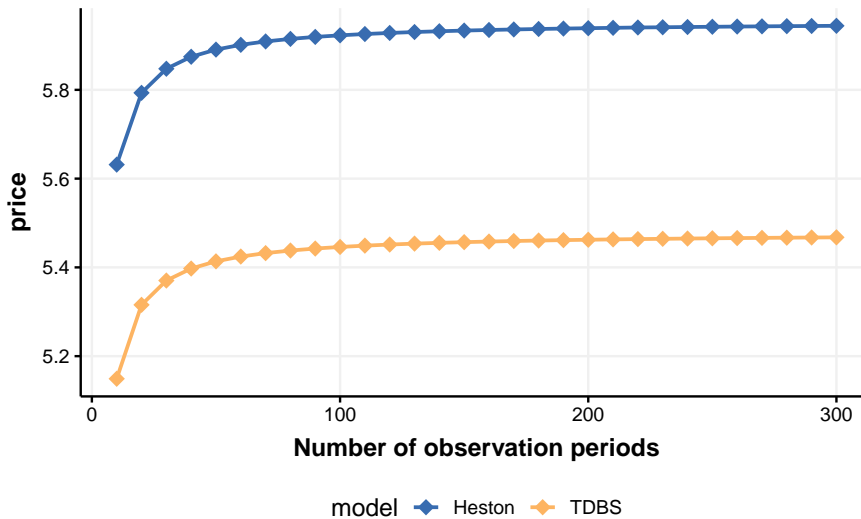


Figure 5.3: Effect of the number of observation periods (N) on the price of a range-accrual for the two market models ($c = 10$, $K^{\text{low}} = 0.9$, $K^{\text{up}} = 1.1$, $T = 1$)

The next parameter is maturity, its effect is illustrated in Figure 5.4. The price of the product is a monotonically decreasing function of maturity in both market models. Regardless of time to maturity, the maximum payout of the product is c , and the coupon accumulation events are stretched to a larger time interval. Payouts further into the future have less probability of being in the $(K^{\text{low}}, K^{\text{up}})$ range, thus decreasing the price. Moreover, if the payouts are further away in time, the effect of discounting will be greater.

The parameters K^{low} , and K^{up} control the size of the range where the product pays coupons. Widening the barrier increases the price, and narrowing it decreases it. If the barrier is set low enough or high enough for the lower and upper barriers, respectively, then

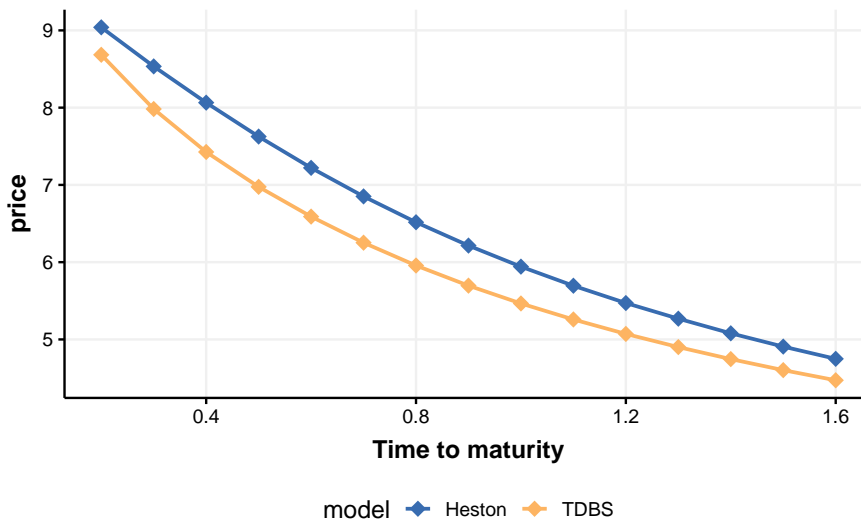


Figure 5.4: Effect of time to maturity on the price of a range-accrual for the two market models ($c = 10$, $N = 250$, $K^{\text{low}} = 0.9$, $K^{\text{up}} = 1.1$)

changes in the parameters have little effect on the price. This is because the underlying has a very low probability of leaving the range. The interesting scenario is when the lower and upper barriers are close to each other. In the left graph of Figure 5.5 the lower barrier is approaching the upper one. In this case, the time-dependent Black Scholes price is higher for low barrier values, but as the upper barrier is approached, the Heston price becomes higher. When the upper barrier is close to the lower one, on the right side of Figure 5.5, the case is reversed. The time-dependent Black-Scholes price is higher until $K^{\text{up}} = 1.05$, where the Heston price becomes higher again. This is due to the distributional differences between the two models. The distribution resulting from the Heston model (with this parameter set) is negatively skewed, while the distribution of the time-dependent Black-Scholes model is lognormal and positively skewed. This is illustrated in Figure 5.6.

As it was mentioned previously, range accruals in equity markets are sometimes issued without an upper barrier. This makes the product more expensive, but the investor can always benefit from a bullish market, as there is no possibility that the asset price will be higher than the upper barrier. The sensitivity to the lower barrier value when the upper barrier is infinity is graphed in Figure 5.7. Increasing the lower barrier value decreases the price of the product. Similarly as before, changing the lower barrier when it is extremely low or extremely high does not affect the price.

The sensitivity analysis was only conducted for the single period range accrual. As the multi-period range accrual is the sum of single period range accruals, the results would not provide an additional understanding of the product.

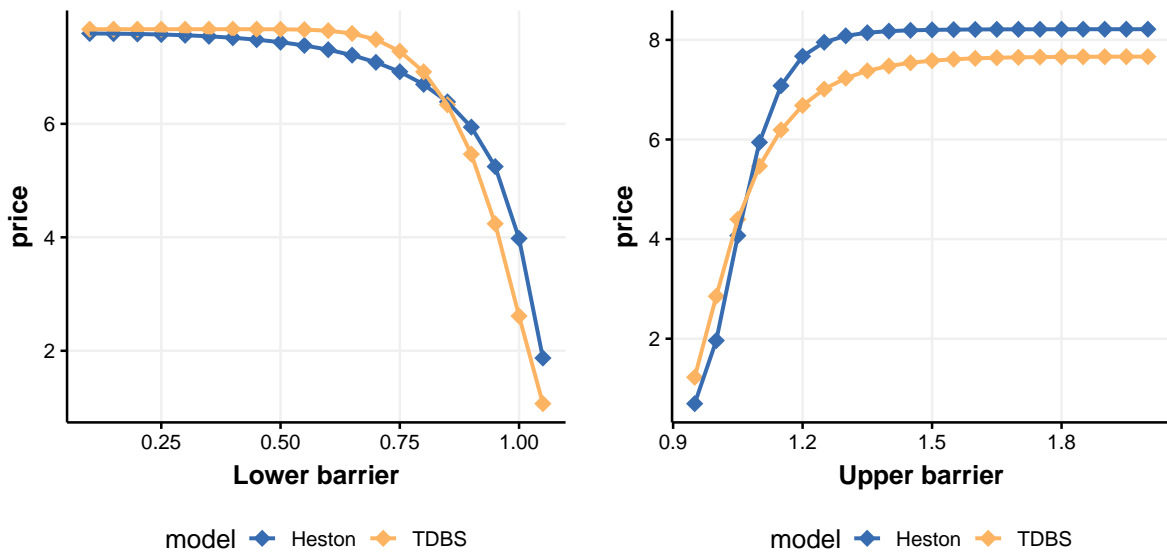


Figure 5.5: Effect of range parameters on the price of a range accrual for the two market models ($c = 10$, $N = 250$, $K^{\text{low}} = 0.9$, $K^{\text{up}} = 1.1$, $T = 1$)

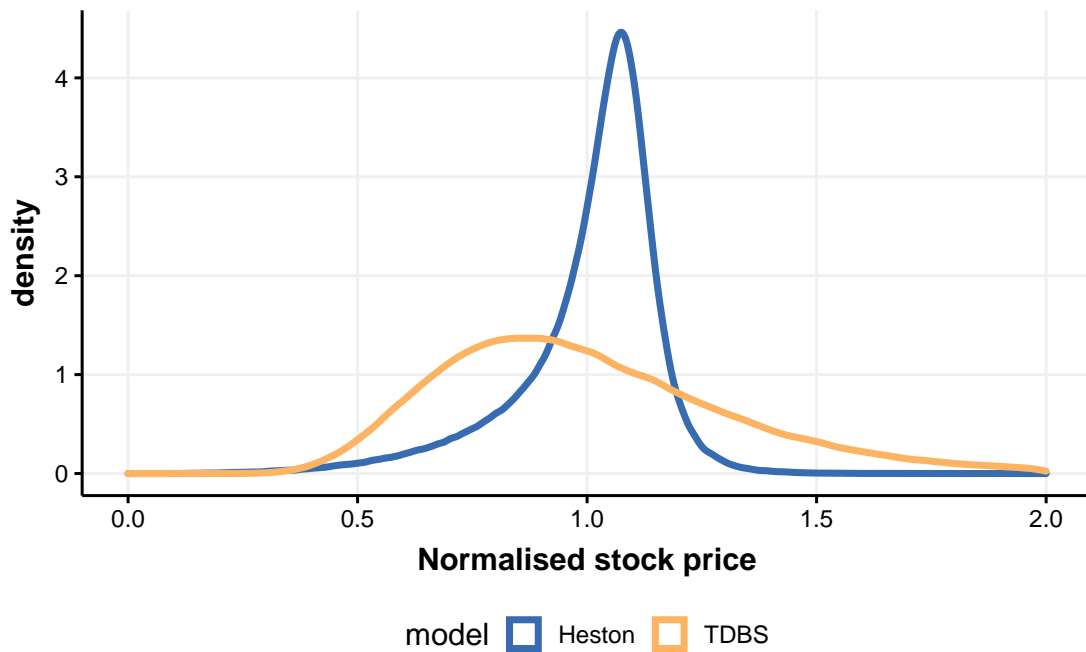


Figure 5.6: Price distribution of the time-dependent Black Scholes and Heston models with the calibrated parameters for $T = 0.5$.

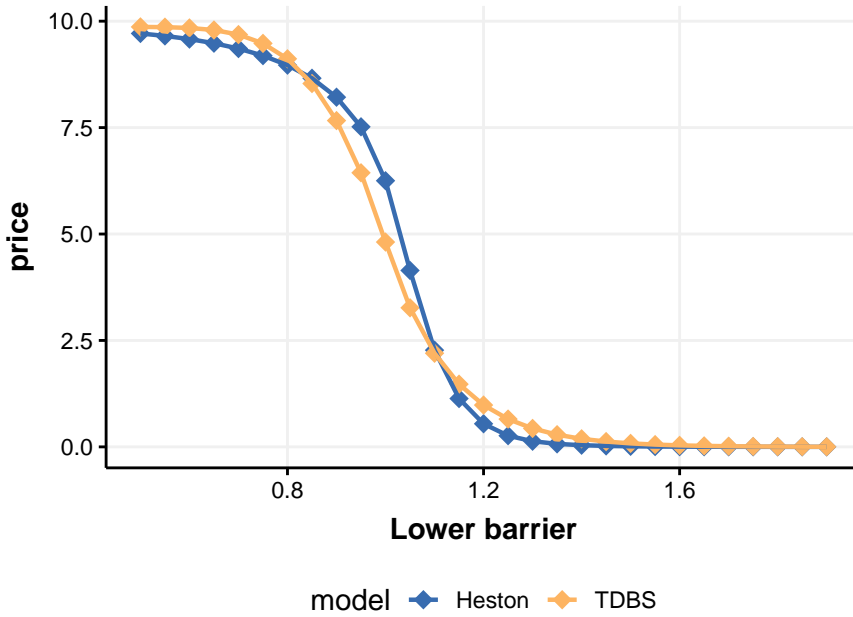


Figure 5.7: Effect of the lower barrier value on the price of a range accrual when there is no upper barrier.

5.3.2 Model parameters

I analyze the effect of changing model parameters of the Heston model. The goal is to observe whether the range accrual reacts to parameter changes in the same manner as the European vanilla option. In this section, the following parameter setup is used.

$$r = 0.1, q = 0, S_0 = 100, v_0 = 0.0625, \theta = 0.04, \kappa = 0.5, \eta = 1, \rho = -0.75$$

To get a complete view of the parameter's effect, the price sensitivity is graphed for different strikes and barrier values. In Figure 5.8, the effect of changing the initial variance is illustrated. For the vanilla call, higher initial variance always results in a higher option price. In the case of the range accrual, for the higher barrier values ($K^{\text{low}} = 1.0, K^{\text{up}} = 1.2$), increasing v_0 has a decreasing effect on the price, but for the other two barrier setups, it increases the price. This can be explained by the shape of the density of the price distribution under the Heston model in Figure A.1 in the appendix. For a low v_0 value, the price distribution is highly concentrated around 1.1², making the price of a range accrual with parameters ($K^{\text{low}} = 1.0, K^{\text{up}} = 1.2$) high. For a larger initial variance, the distribution is more dispersed, which decreases the price for the ($K^{\text{low}} = 1.0, K^{\text{up}} = 1.2$) case, but increases it for the other two barrier setups.

The effect of the speed of mean reversion is graphed for two cases: When the initial variance is greater than the long-run average and vice versa. In the case of the range

²For this specific parameter setup.

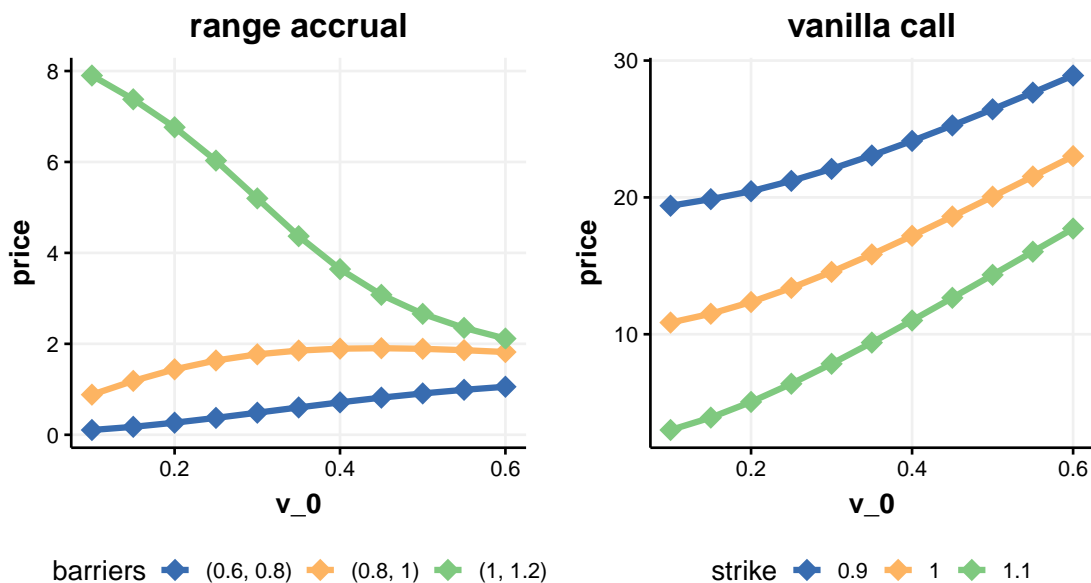


Figure 5.8: Effect of the v_0 parameter on the price of a range-accrual and the price of a vanilla call option (The x-axis is the initial volatility, $\sqrt{v_0}$)

accrual, increasing the speed of mean reversion decreases the price when $v_0 < \theta$ and increases it when $v_0 > \theta$. For the vanilla option, the effect is reversed. The density function of the $v_0 > \theta$ case is graphed in Figure [A.2](#) in the appendix. For larger κ , values the density function shifts to the right, which increases the price of the vanilla option, but because the range accrual does not accumulate coupon if the stock price is above $K^{\text{up}} = 1.2$, its price is decreased. If $v_0 < \theta$, the reverse is true, the density function shifts to the left, increasing the price of the range accrual while decreasing the price of the vanilla option.

Sensitivity to the volatility of variance parameter η is graphed in Figure [5.10](#). An increase in η results in lower option prices for the vanilla call. This is a bit counter-intuitive, as one would think that an increase in the volatility of variance would also increase the price of the vanilla call. As previously, the effect can be understood if we take a look at the densities in Figure [A.3](#) in the appendix. An increase in η makes the distribution heavier tailed, but the probability of the stock price being in the (1.2, 2) range decreases. Similarly, as before the η sensitivity of the range accrual depends on the barrier values. For the ($K^{\text{low}} = 1.0$, $K^{\text{up}} = 1.2$) version, an increase in the volatility of variance increases the price, but for the other barrier setups, it decreases it.

The effect of other model parameters can be seen in Figure [A.4](#) in the appendix. The results are very similar, thus, they were put into the appendix to avoid the crowding of images. Parameter changes in the Heston model have a different effect on the range accrual depending on the barrier setups as before. In the case of the vanilla call option an

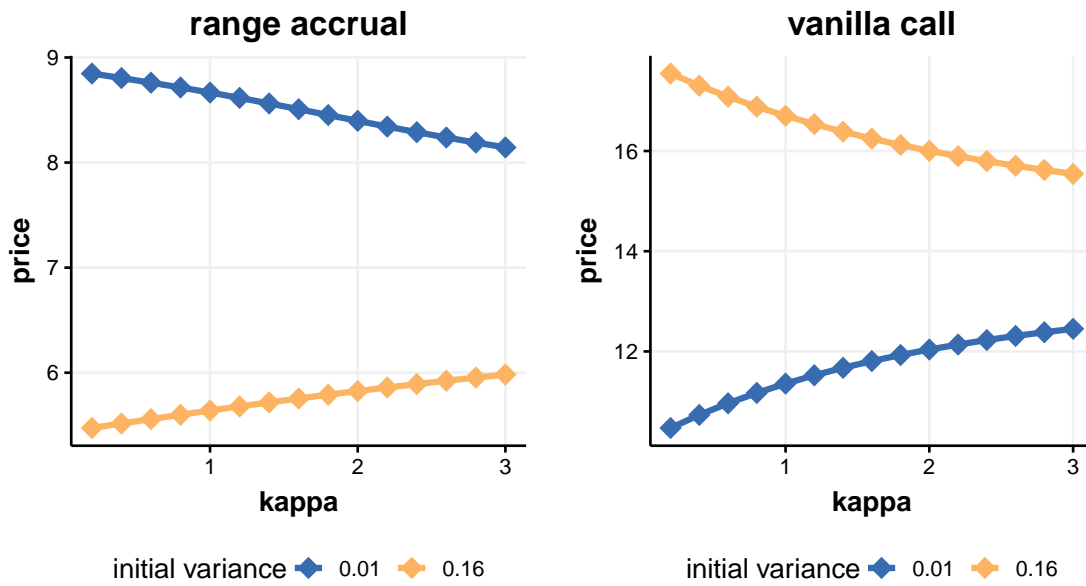


Figure 5.9: Effect of the κ parameter on the price of a range accrual and the price of a vanilla call option ($\theta = 0.04$)

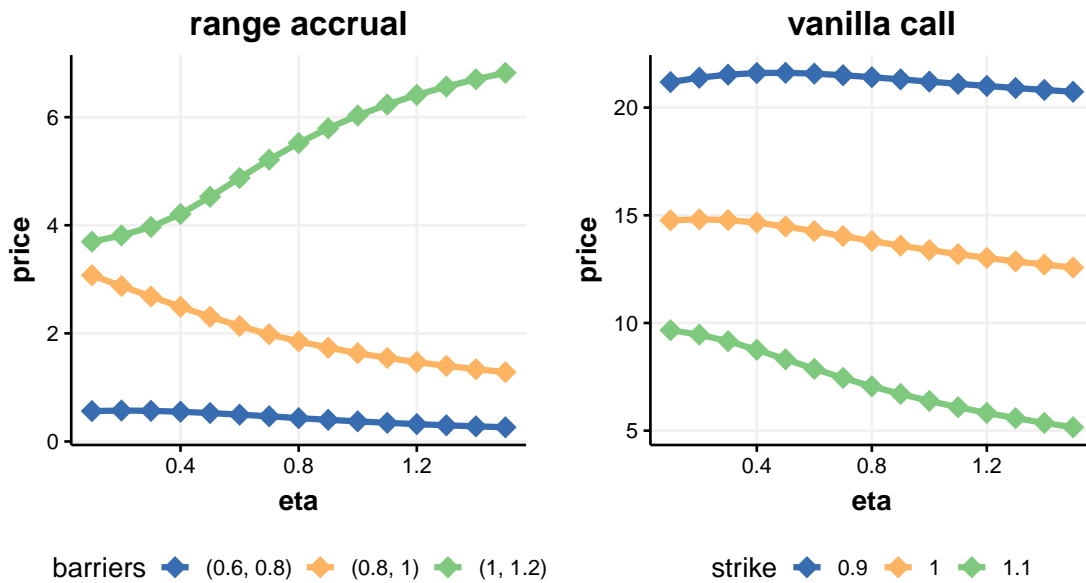


Figure 5.10: Effect of the η parameter on the price of a range accrual and the price of a vanilla call option.

increase in θ increases the price, because the average volatility will be higher. An increase in the correlation decreases the price.

From these results, it is apparent that the range accrual reacts to parameter changes differently than the vanilla call option. This supports the proposal that was made earlier,

that the Heston model should be calibrated to range accrual prices instead of vanilla option prices. Moreover, the calibration process should be done separately for different K^{low} and K^{up} barrier values, because the behaviour of prices is highly dependent on these barriers. This is unfortunately not feasible due to the lack of quoted market prices, mentioned in Section [2.2](#).

Chapter 6

Summary

The aim of this thesis was to give a thorough description of range accrual products written on equity underliers, including the pricing methodology and calibration process. A range accrual is a derivative that accumulates coupons when the underlying is quoted in a specified range, and pays it out at the end of the coupon determination period. Essentially, the investor bets that the price of an asset will not leave the range. It is a very flexible product that can be tailored to match a vast range of market views, let it be bearish or bullish. It is widely used in several different markets, such as interest rates, foreign exchange and equity. I was motivated to research this topic because I found that equity-linked range accruals are less researched than their interest rate-linked counterparts, and I wanted to see how equity-linked range accruals could be modeled and priced.

First, I introduced the payoff structure of the product and reviewed the surrounding literature. After that, I gave an overview of the models that are usually used for pricing equity-linked derivatives. Two families of models were discussed: deterministic volatility models and stochastic volatility models. Several models were listed from each category, including the local volatility model, diffusion stochastic volatility models and jump-diffusion models. Finally, I settled on two models for the rest of the analysis: the time-dependent Black-Scholes model and the Heston model. Formulas for the vanilla call option and the digital option were given in both models. The calibration process was also discussed. The time-dependent Black-Scholes model could be calibrated analytically if volatility is assumed to be a piecewise constant function. On the other hand, the five parameters of the Heston model needed to be calibrated numerically to market data.

The main result of range accrual pricing is that the price of the product can be broken down into a series of range digital options with delayed payoffs. At each date when the range accrual could accumulate a coupon, the buyer essentially has a digital option with payoff delayed to the end of the coupon determination period. The digital option has a closed-form formula in the time-dependent Black-Scholes model and a semi-closed-form

solution in the Heston model. As a result, the pricing could be done analytically, without the need for Monte Carlo simulations.

In the last part of the thesis, I implemented the pricing and calibration of the above-mentioned two models in the R programming language. The calibration process is important because it does not matter how efficient the pricing is, if the model can not fit the market data. Both models were calibrated to vanilla call options on the S&P500 index. It was found that the Heston model could fit the data much better than the time-dependent Black-Scholes model. However, in the low time to maturity case, even the Heston model seemed to be unable to match the high curvature of the market-implied volatility smile. Lastly, the sensitivity to both the product and model parameters was examined. The sensitivity analysis showed that the price of the range accrual reacts to changes in the Heston model parameters quite differently than the price of a vanilla call option. From this result, I concluded that the calibration to vanilla call prices is not sufficient, the range accrual should be calibrated to quoted range accrual prices. This kind of data is not available to the public, but in the industry, there are possibilities to obtain it.

As part of a future research, different market models could be implemented and compared. It would be particularly interesting to compare the local volatility model to the stochastic local volatility model. As both models can fit the market prices perfectly, it could be examined how stochastic volatility affects range accrual prices. Another area of research could be to examine the prices of range accruals with exotic features, such as the callable range accrual or the floating rate range accrual.

Bibliography

- Aït-Sahalia, Y., & Lo, A. W. (1998). Nonparametric estimation of state-price densities implicit in financial asset prices. *The journal of finance*, *53*(2), 499–547.
- Barndorff-Nielsen, O. E., & Shephard, N. (2001). Non-gaussian ornstein–uhlenbeck-based models and some of their uses in financial economics. *Journal of the Royal Statistical Society: Series B (Statistical Methodology)*, *63*(2), 167–241.
- Bates, D. S. (1996). Jumps and stochastic volatility: Exchange rate processes implicit in deutsche mark options. *The Review of Financial Studies*, *9*(1), 69–107.
- Baxter, M., Rennie, A., & Rennie, A. J. (1996). *Financial calculus: An introduction to derivative pricing*. Cambridge university press.
- Black, F., & Scholes, M. S. (1973). The Pricing of Options and Corporate Liabilities. *Journal of Political Economy*, *81*(3), 637–654. <https://doi.org/10.1086/260062>
- Brigo, D., Morini, M., & Pallavicini, A. (2013). *Counterparty credit risk, collateral and funding: With pricing cases for all asset classes* (Vol. 478). John Wiley & Sons.
- Buraschi, A., & Jackwerth, J. (2001). The price of a smile: Hedging and spanning in option markets. *The Review of Financial Studies*, *14*(2), 495–527.
- Byrd, R. H., Lu, P., Nocedal, J., & Zhu, C. (1995). A limited memory algorithm for bound constrained optimization. *SIAM Journal on scientific computing*, *16*(5), 1190–1208.
- Chan, R. H., Guo, Y. Z., Lee, S. T., & Li, X. (2019). *Financial mathematics, derivatives and structured products*. Springer.
- Chiarella, C., Da Fonseca, J., & Grasselli, M. (2014). Pricing range notes within wishart affine models. *Insurance: Mathematics and Economics*, *58*, 193–203.
- Cox, J. C., Ingersoll Jr, J. E., & Ross, S. A. (1985). A theory of the term structure of interest rates. *Econometrica*, *53*(2), 385–408.
- Duffie, D., Pan, J., & Singleton, K. (2000). Transform analysis and asset pricing for affine jump-diffusions. *Econometrica*, *68*(6), 1343–1376.
- Dupire, B. (1994). Pricing with a smile. *Risk*, *7*(1), 18–20.
- Faraj, K., & Khaled, A. (2019). *Sure time to grasp the potential of structured products*. Retrieved February 9, 2022, from <https://www.bloomberg.com/professional/blog/sure-time-to-grasp-the-potential-of-structured-products/>
- Gatheral, J. (2011). *The volatility surface: A practitioner’s guide*. John Wiley & Sons.

- Heath, D., Jarrow, R., & Morton, A. (1992). Bond pricing and the term structure of interest rates: A new methodology for contingent claims valuation. *Econometrica: Journal of the Econometric Society*, 77–105.
- Heston, S. L. (1993). A closed-form solution for options with stochastic volatility with applications to bond and currency options. *The review of financial studies*, 6(2), 327–343.
- HochSchule RheinMain. (n.d.). The Time-Dependent Black-Scholes Model and Calibration to Market [University lecture note].
- Huang, H. (2011). Pricing range accrual notes in an affine term structure model with stochastic mean, stochastic volatility and jump. *SSRN Electronic Journal*. <https://doi.org/10.2139/ssrn.1917415>
- Hull, J. (2012). *Risk management and financial institutions, + web site* (Vol. 733). John Wiley & Sons.
- Hull, J., & White, A. (1987). The pricing of options on assets with stochastic volatilities. *The journal of finance*, 42(2), 281–300.
- Lazar, V. L. (2003). Pricing digital call option in the heston stochastic volatility model. *Studia Univ. Babeş-Bolyai Math*, 48(3), 83–92.
- Lewis, A. L. (2019). Heston model reference prices. <https://financepress.com/2019/02/15/heston-model-reference-prices/>
- Li, S., Huang, H. H., & Zhang, T. (2020). Generalized affine transform on pricing quanto range accrual note. *The North American Journal of Economics and Finance*, 54, 100892.
- Liao, S.-L., & Hsu, P.-P. (2009). Pricing and hedging of quanto range accrual notes under gaussian hjm with cross-currency levy processes. *Journal of Futures Markets: Futures, Options, and Other Derivative Products*, 29(10), 973–998.
- Lin, S.-K., Wang, S.-Y., Chen, C. R., & Xu, L.-W. (2017). Pricing range accrual interest rate swap employing libor market models with jump risks. *The North American Journal of Economics and Finance*, 42, 359–373.
- Madan, D. B., & Seneta, E. (1990). The variance gamma (vg) model for share market returns. *Journal of business*, 511–524.
- Márkus, L. (2017). Eszközár folyamatok modellezése, valamint európai és amerikai opciók árazása (egyetemi jegyzet).
- Merton, R. C. (1976). Option pricing when underlying stock returns are discontinuous. *Journal of financial economics*, 3(1-2), 125–144.
- Mijatović, A., & Tankov, P. (2016). A new look at short-term implied volatility in asset price models with jumps. *Mathematical Finance*, 26(1), 149–183.
- Mrázek, M., & Pospíšil, J. (2017). Calibration and simulation of heston model. *Open Mathematics*, 15(1), 679–704.

- Navatte, P., & Quittard-Pinon, F. (1999). The valuation of interest rate digital options and range notes revisited. *European Financial Management*, 5(3), 425–440.
- Nunes, J. P. V. (2004). Multifactor valuation of floating range notes. *Mathematical Finance: An International Journal of Mathematics, Statistics and Financial Economics*, 14(1), 79–97.
- Oosterlee, C. W., & Grzelak, L. A. (2019). *Mathematical modeling and computation in finance: With exercises and python and matlab computer codes*. World Scientific.
- Rubinstein, M. (1994). Implied binomial trees. *The journal of finance*, 49(3), 771–818.
- Said, K. (1999). Pricing exotics under the smile. *RISK-LONDON-RISK MAGAZINE LIMITED-*, 12, 72–75.
- Saporito, Y. F., Yang, X., & Zubelli, J. P. (2019). The calibration of stochastic local-volatility models: An inverse problem perspective. *Computers & Mathematics with Applications*, 77(12), 3054–3067.
- Scott, L. O. (1987). Option pricing when the variance changes randomly: Theory, estimation, and an application. *Journal of Financial and Quantitative analysis*, 22(4), 419–438.
- Shu, J., & Zhang, J. E. (2004). Pricing s&p 500 index options under stochastic volatility with the indirect inference method. *Journal of derivatives accounting*, 1(02), 171–186.
- Stein, E. M., & Stein, J. C. (1991). Stock price distributions with stochastic volatility: An analytic approach. *The review of financial studies*, 4(4), 727–752.
- Tan, C. (2010). *Demystifying exotic products: Interest rates, equities and foreign exchange*. John Wiley & Sons.
- Thompson, S. (2011). The stylised facts of stock price movements. *The New Zealand Review of Economics and Finance*, 1.
- Turnbull, S. M. (1995). Interest rate digital options and range notes. *The Journal of Derivatives*, Fall.
- Vörös, L. (2018). *A volatilitásmosoly fedezésének vizsgálata a részvénypiacon* (Master's thesis). Budapesti Corvinus Egyetem.

Appendix A

Proofs and figures

A.1 Proofs

A.1.1 Modification of the Black-Scholes formula for the time-dependent case

To find this modificationb consider the log return process of a time-dependent Black-Scholes model, denoted by X_t

$$dX_t = \left(\mu - \frac{1}{2}\sigma^2(t) \right) dt + \sigma(t)dW_t \quad (\text{A.1})$$

Its expected value is

$$\mathbb{E}[X_T] = X_0 + \int_0^T \left(\mu - \frac{1}{2}\sigma^2(t) \right) dt \quad (\text{A.2})$$

and the variance is

$$\mathbb{D}^2[X_T] = \mathbb{E} \left[\int_0^T \sigma(t)dW_t \right]^2 = \int_0^T \sigma^2(t)dt \quad (\text{A.3})$$

Let us consider another log return process $Y(t)$, which has constant volatility denoted by σ_*

$$dY_t = \left(\mu - \frac{1}{2}\sigma_*^2 \right) dt + \sigma_*dW_t \quad (\text{A.4})$$

Its expected value and variance are given similarly

$$\mathbb{E}[Y_T] = Y_0 + \left(\mu - \frac{1}{2}\sigma_*^2 \right) T \quad \mathbb{D}^2[Y_T] = \sigma_*^2 T \quad (\text{A.5})$$

We are searching for a volatility parameter σ_* for which both the expected values and the variance of the processes are the same. By equating the two variances in equations [A.3](#) and [A.5](#), we get

$$\sigma_* = \sqrt{\frac{1}{T} \int_0^T \sigma^2(t)dt} \quad (\text{A.6})$$

This value of σ_* also makes the expected value of the two processes equal if $X_0 = Y_0$

$$\begin{aligned} \mathbb{E}[Y(T)] &= Y_0 + \left(\mu - \frac{1}{2}\sigma_*^2 \right) T \\ &= X_0 + \left(\mu - \frac{1}{2} \frac{1}{T} \int_0^T \sigma^2(t) dt \right) T = \mathbb{E}[X(T)] \end{aligned} \quad (\text{A.7})$$

Because X_t and Y_t are normally distributed, the first two matching moments guarantee equality in distribution.

A.1.2 Formula for the European vanilla call option under the Heston model

I follow (Gatheral, 2011) in deriving the price of a vanilla call option under the Heston model. To get the price of the vanilla European call option, the PDE in equation 4.30 needs to be solved with the boundary condition

$$V(T, S, v) = (S_T - K)^+ \quad (\text{A.8})$$

Let $F_{t,T}$ be the time T forward price of the stock and introduce the new variable $x = F_{t,T}/K$. Moreover, let us define $\tau = T - t$, and consider the derivative's future value to expiration instead its present value. This is denoted by $C(x, v, \tau)$. Rewriting equation 4.30 in terms of $C(x, v, \tau)$ simplifies the PDE to

$$-\frac{\partial C}{\partial \tau} + \frac{1}{2}v \frac{\partial^2 C}{\partial x^2} - \frac{1}{2}v \frac{\partial C}{\partial x} + \frac{1}{2}\eta^2 v \frac{\partial^2 C}{\partial v^2} + \rho\eta v \frac{\partial^2 C}{\partial x \partial v} - \kappa(v - \theta) \frac{\partial C}{\partial v} = 0 \quad (\text{A.9})$$

where the subscripts x and v refer to differentiating C with respect to the subscript. As stated in (Duffie et al., 2000) the solution to equation A.9 has the general form

$$C(x, v, \tau) = K \{ e^x P_1(x, v, \tau) - P_0(x, v, \tau) \} \quad (\text{A.10})$$

Similarly to the Black-Scholes formula, the first term in the brackets (P_1) represents the pseudo-expectation of the final index level given that the option is in-the-money and the second term (P_0) represents the pseudo-probability of exercise.

Substituting in the proposed solution, to equation A.9, we get equations governing P_0 and P_1

$$-\frac{\partial P_j}{\partial \tau} + \frac{1}{2}v \frac{\partial^2 P_j}{\partial x^2} - \left(\frac{1}{2} - j \right) v \frac{\partial P_j}{\partial x} + \frac{1}{2}\eta^2 v \frac{\partial^2 P_j}{\partial v^2} + \rho\eta v \frac{\partial^2 P_j}{\partial x \partial v} + (a - b_j v) \frac{\partial P_j}{\partial v} = 0 \quad (\text{A.11})$$

for $j = 0, 1$ and

$$a = \kappa\theta \quad b_j = \kappa - j\rho\eta$$

subject to the terminal condition

$$\lim_{\tau \rightarrow 0} P_j(x, v, \tau) = \begin{cases} 1 & \text{if } x > 0 \\ 0 & \text{if } x \leq 0 \end{cases} := \lambda(x) \quad (\text{A.12})$$

To solve equation [A.11](#) with terminal condition [A.12](#), a Fourier transform technique is used. Let us define the Fourier transform of P_j as

$$\tilde{P}(u, v, \tau) = \int_{-\infty}^{\infty} e^{-iux} P(x, v, \tau) dx \quad (\text{A.13})$$

which at $\tau = 0$ evaluates to

$$\tilde{P}(u, v, 0) = \int_{-\infty}^{\infty} e^{-iux} \lambda(x) dx = \frac{1}{iu} \quad (\text{A.14})$$

The inverse transform is

$$P(x, v, \tau) = \int_{-\infty}^{\infty} \frac{1}{2\pi} e^{iux} \tilde{P}(u, v, \tau) du \quad (\text{A.15})$$

The Fourier transform is applied to equation [A.11](#). This cancels out the derivatives with respect to x .

$$-\frac{\partial \tilde{P}_j}{\partial \tau} - \frac{1}{2} v u^2 \tilde{P}_j - \left(\frac{1}{2} - j\right) i u v \tilde{P}_j + \frac{1}{2} \eta^2 v \frac{\partial^2 \tilde{P}_j}{\partial v^2} + \rho \eta i u v \frac{\partial \tilde{P}_j}{\partial v} + (a - b_j v) \frac{\partial \tilde{P}_j}{\partial v} = 0 \quad (\text{A.16})$$

Now define the variables

$$\begin{aligned} \alpha &= -\frac{u^2}{2} - \frac{i u}{2} + i j u \\ \beta &= \theta - \rho \eta j - \rho \eta i u \\ \gamma &= \frac{\eta^2}{2} \end{aligned}$$

With these variables, equation [A.16](#) becomes

$$v \left\{ \alpha \tilde{P}_j - \beta \frac{\partial \tilde{P}_j}{\partial v} + \gamma \frac{\partial^2 \tilde{P}_j}{\partial v^2} \right\} + a \frac{\partial \tilde{P}_j}{\partial v} - \frac{\partial \tilde{P}_j}{\partial \tau} = 0 \quad (\text{A.17})$$

because of the Heston characteristic function¹ \tilde{P}_j has the form

$$\begin{aligned} \tilde{P}_j(u, b, \tau) &= \exp\{C(u, \tau)\theta + D(u, \tau)v\} \tilde{P}_j(u, v, 0) \\ &= \frac{1}{iu} \exp\{C(u, \tau)\theta + D(u, \tau)v\} \end{aligned} \quad (\text{A.18})$$

From this, the partial derivatives of \tilde{P}_j are as follows

$$\begin{aligned} \frac{\partial \tilde{P}_j}{\partial \tau} &= \left\{ \theta \frac{\partial C}{\partial \tau} + v \frac{\partial D}{\partial \tau} \right\} \tilde{P}_j \\ \frac{\partial \tilde{P}_j}{\partial v} &= D \tilde{P}_j \\ \frac{\partial^2 \tilde{P}_j}{\partial v^2} &= D^2 \tilde{P}_j \end{aligned}$$

¹see (Gatheral, [2011](#)) for the derivation of the characteristic function

Equation [A.17](#) is satisfied if

$$\begin{aligned}\frac{\partial C}{\partial \tau} &= \theta D \\ \frac{\partial D}{\partial \tau} &= \alpha - \beta D + \gamma D^2 \\ &= \gamma(D - r_+)(D - r_-)\end{aligned}\tag{A.19}$$

where r_{\pm} is defined to be

$$r_{\pm} = \frac{\beta \pm \sqrt{\beta^2 - 4\alpha\gamma}}{2\gamma} =: \frac{\beta \pm d}{\eta^2}$$

Integrating $C(u, \tau)$ and $D(u, \tau)$ in equation [A.19](#) with terminal condition $C(u, 0) = 0$, $D(u, 0) = 0$ yields

$$\begin{aligned}D(u, \tau) &= r_- \frac{1 - e^{-d\tau}}{1 - ge^{-d\tau}} \\ C(u, \tau) &= \theta \left\{ r_{\tau} - \frac{2}{\eta^2} \log \left(\frac{1 - e^{-d\tau}}{1 - g} \right) \right\}\end{aligned}\tag{A.20}$$

where g is defined as

$$g := \frac{r_-}{r_+}$$

Now that $C(u, \tau)$ and $D(u, \tau)$ are identified, they can be substituted to equation [A.18](#). From there, the inverse Fourier transformation can be applied, and the pseudo-probabilities P_j will be given in the form of an integral of a real-valued function.

$$P_j(x, v, \tau) = \frac{1}{2} + \frac{1}{\pi} \int_0^{\infty} \operatorname{Re} \left\{ \frac{\exp\{C_j(u, \tau)\theta + D_j(u, \tau)v + iux\}}{iu} \right\} du\tag{A.21}$$

A.1.3 Almost exact simulation of the Heston model

As a reminder, the dynamics of the log return process $X_t = \log S_t$ is

$$dX_t = \left(\mu - \frac{1}{2}v_t\right)dt + \sqrt{v_t}dW_t^1\tag{A.22}$$

$$dv_t = \kappa(\theta - v_t)dt + \eta\sqrt{v_t}dW_t^2\tag{A.23}$$

This can be expressed with independent Wiener processes W_t^A and W_t^B combining them according to the Cholesky factorization.

$$dX_t = \left(\mu - \frac{1}{2}v_t\right)dt + \sqrt{v_t} \left[\rho dW_t^A + \sqrt{1 - \rho^2} dW_t^B \right]\tag{A.24}$$

$$dv_t = \kappa(\theta - v_t)dt + \eta\sqrt{v_t}dW_t^A\tag{A.25}$$

Let us integrate the processes in a given interval $[t_i, t_{i+1}]$

$$X_{i+1} = X_i + \int_{t_i}^{t_{i+1}} \left(\mu - \frac{1}{2}v_t\right)dt + \rho \int_{t_i}^{t_{i+1}} \sqrt{v_t}dW_t^A + \sqrt{1 - \rho^2} \int_{t_i}^{t_{i+1}} \sqrt{v_t}dW_t^B \quad (\text{A.26})$$

$$v_{i+1} = v_i + \kappa \int_{t_i}^{t_{i+1}} (\theta - v_t)dt + \eta \int_{t_i}^{t_{i+1}} \sqrt{v_t}dW_t^A \quad (\text{A.27})$$

It can be noticed that the term $\int_{t_i}^{t_{i+1}} \sqrt{v_t}dW_t^A$ appears in both equations, and it can be expressed as

$$\int_{t_i}^{t_{i+1}} \sqrt{v_t}dW_t^A = \frac{1}{\eta} \left(v_{i+1} - v_i - \kappa \int_{t_i}^{t_{i+1}} (\theta - v_t)dt \right) \quad (\text{A.28})$$

This is useful because the stochastic integral on the left side of equation [A.28](#) is expressed through $v_{i+1} - v_i$, which can be simulated from the noncentral chi-square distribution, and an integral with respect to time, which can be approximated. Using this, the value of X_{i+1} can be written as

$$\begin{aligned} X_{i+1} = X_i + \int_{t_i}^{t_{i+1}} \left(\mu - \frac{1}{2}v_t\right)dt + \frac{\rho}{\eta} \left(v_{i+1} - v_i - \kappa \int_{t_i}^{t_{i+1}} (\theta - v_t)dt \right) \\ + \sqrt{1 - \rho^2} \int_{t_i}^{t_{i+1}} \sqrt{v_t}dW_t^B \end{aligned} \quad (\text{A.29})$$

We can approximate the integrals by fixing the integrand at its left boundary value, similarly to Euler's method.

$$\begin{aligned} X_{i+1} \approx X_i + \int_{t_i}^{t_{i+1}} \left(\mu - \frac{1}{2}v_i\right)dt + \frac{\rho}{\eta} \left(v_{i+1} - v_i - \kappa \int_{t_i}^{t_{i+1}} (\theta - v_i)dt \right) \\ + \sqrt{1 - \rho^2} \int_{t_i}^{t_{i+1}} \sqrt{v_i}dW_t^B \end{aligned} \quad (\text{A.30})$$

A.2 Figures

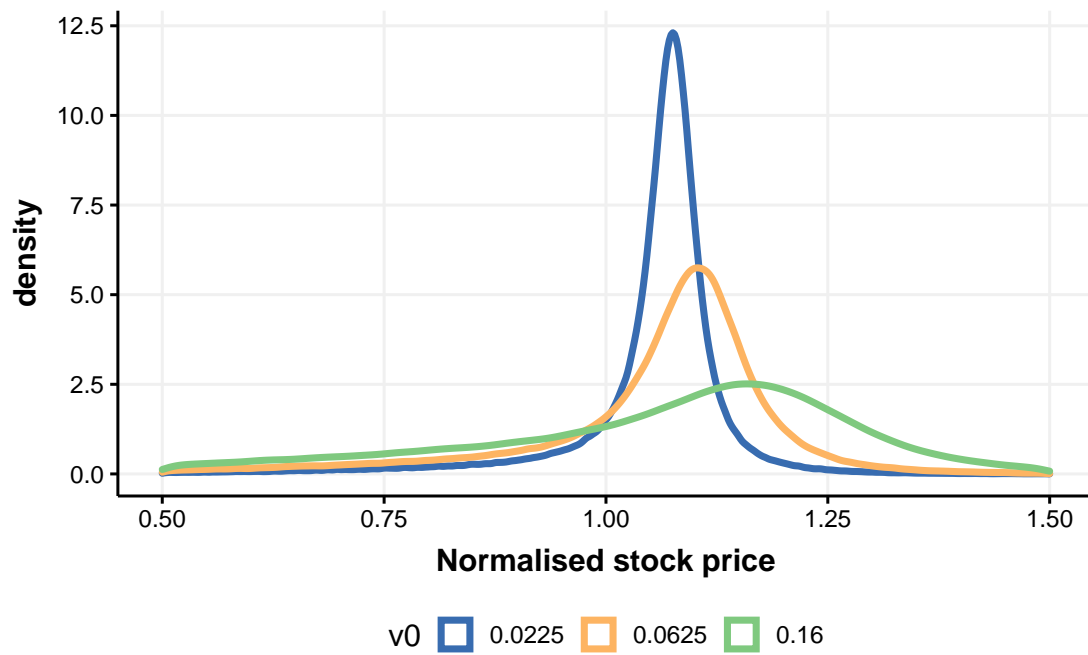


Figure A.1: Price distribution of the Heston model for different v_0 parameters

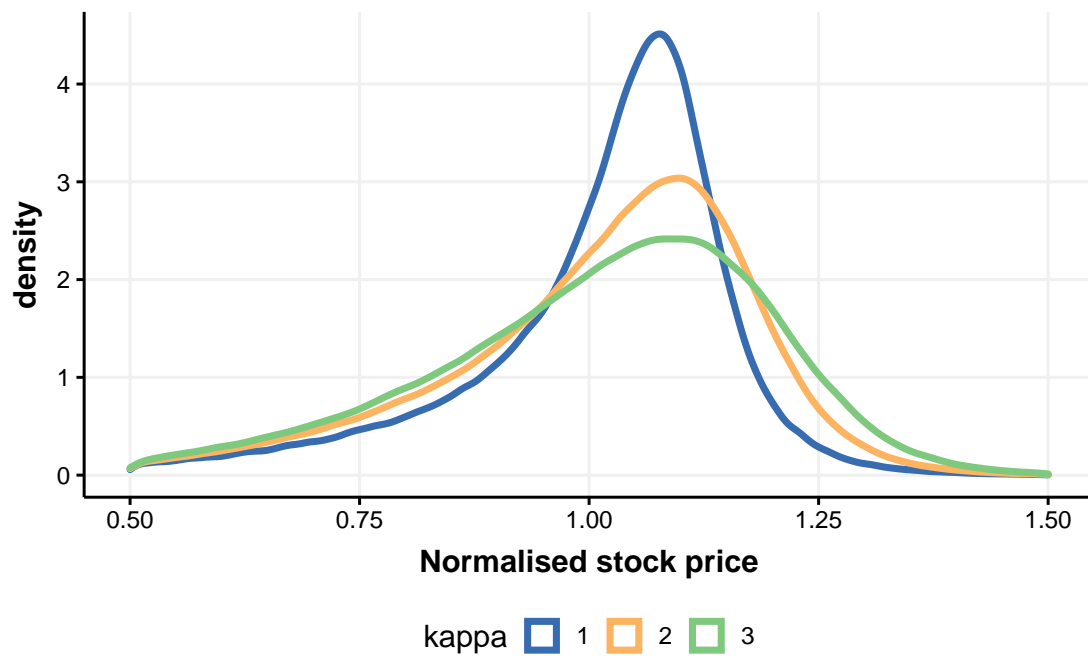


Figure A.2: Price distribution of the Heston model for different κ parameters

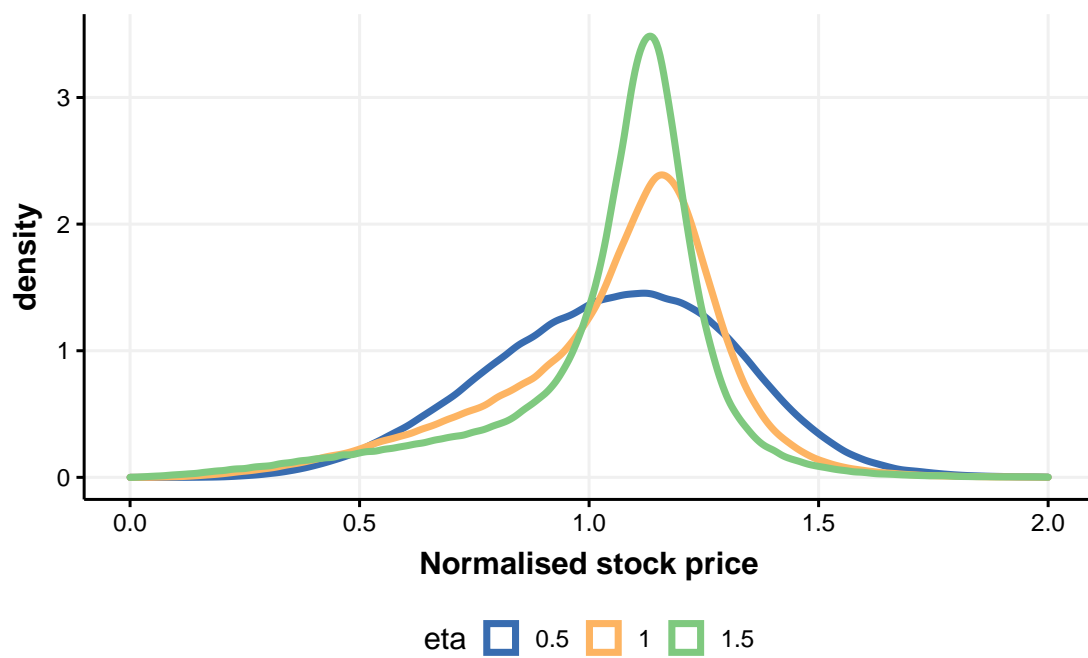


Figure A.3: Price distribution of the Heston model for different η parameters

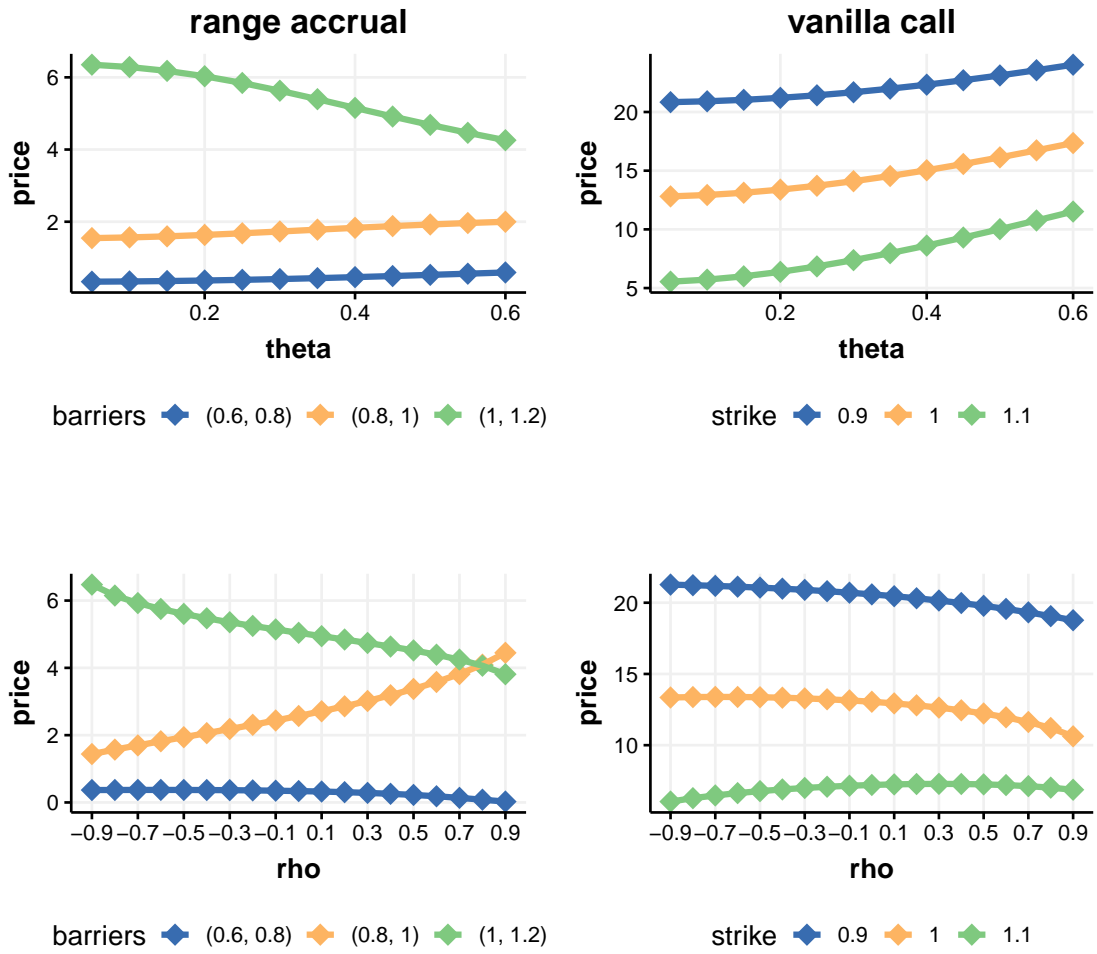


Figure A.4: Effect of the θ , and ρ parameters on the price of a range accrual and the price of a vanilla call option

Appendix B

R code

The code used in the empirical results chapter can be found on the following [github link](#), or at the url <https://github.com/papkri/pricing-range-accrual-products>. Here, I will explain the most important functions.

- **callHestoncf** and **callHestoncf_digital**

It calculates the Heston price of a vanilla call option and a digital option , respectively. The function uses numerical integration to evaluate the formula in Theorems [7](#) and [8](#).

- **sRAN_analytic**

Calculates the price of a single period range accrual in the Heston model. The price is calculated as the sum of range digital options with delayed payments. Each digital option price is calculated by **callHestoncf_digital**.

- **BSTD_vanilla** and **BSTD_digital**

Calculates the price of a vanilla call option and a digital option in the time-dependent Black-Scholes model. The function assumes that volatility is a piecewise constant function and expects a vector of volatility values, and a vector of time values when the volatility function changes.

- **sRAN_analytic_TDBS**

Calculates the price of a single period range accrual in the time-dependent Black-Scholes model. The price is calculated as the sum of range digital options with delayed payments. Each digital option price is calculated by **BSTD_digital**.

- **Heston_calibrator_multiMat**

Function for calibrating the Heston model with the limited-memory BFGS method.

- **CIR_sample** and **Heston_paths_AE**

The function **CIR_sample** generates the next step of the CIR variance process based on equations [4.40](#) and [4.41](#), conditioning on the vector of previous variances. The **Heston_paths_AE** function generates sample paths of the Heston model based on equations [4.42](#) and [4.43](#).

Összefoglalás

A szakdolgozat célja, hogy bemutassa a sávós hozamfelhalmozó (range accrual) termékeket, beleértve az árazást és a kalibrációs folyamatot. A sávós hozamfelhalmozó olyan termék amely kuponokat halmoz fel, ha az alaptermék egy előre meghatározott sávon belül tartózkodik. A gyakorlatban általában napi gyakorisággal megfigyelik, hogy az alaptermék az adott napon a sávon belül tartózkodott-e, és ha igen, akkor a termék felhalmozza a kupont arra a napra. A kupongyűjtési időszak végén kifizetésre kerülnek az addig felhalmozott kuponok. A terméknek lehet egy vagy akár több kupongyűjtési időszaka is, és amennyiben több időszakkal rendelkezik, mindegyik végén történik kifizetés. Ezek a termékek több különböző piacon is elterjedtek, azonban a dolgozatban olyan sávós hozamfelhalmozó termékeket vizsgálok, amiknek alapterméke részvény. A dolgozatban a saját hozzájárulás az árazás és kalibráció implementációja az R programnyelvben, illetve a termék érzékenységvizsgálata.

A szakdolgozat első fejezetében bemutatom a sávós hozamfelhalmozó termékek kifizetését, kitérve arra is, hogy milyen egzotikus kiegészítései vannak a terméknek. Ezután áttekintem a termék szakirodalmát. Az irodalomban (Turnbull, 1995) és (Navatte & Quittard-Pinon, 1999) cikkjei tekinthetők kiindulási alapnak. Ezen cikkek szerzői levezetik, hogyan lehet a sávós hozamfelhalmozó árát visszavezetni bináris opciók összegére. Minden alkalommal amikor a termék kupont halmozhat fel, a befektető valójában egy bináris opcióval rendelkezik, aminek a kifizetése el van tolvá a kupongyűjtési időszak végére. Ez jóval egyszerűbb árazást tesz lehetővé, a dolgozat későbbi részében én is ezt a megközelítést implementálom. A szakirodalom nagyrésze, beleértve az előbbi két cikket is, a kamatlábak piacán vizsgálják a termék árazását. Mivel a szakdolgozat a részvényhez kötött sávós hozamfelhalmozókat vizsgálja, ezért áttekintettem a részvénypiacok modellezésének szakirodalmát is. A főbb források amiket a témában felhasználtam a klasszikusnak mondható (Gatheral, 2011) könyv a volatilitásfelületről, és (Oosterlee & Grzelak, 2019) könyve a matematikai modellezésről.

A következő fejezetben részletesen tárgyaltam a részvénypiacok modellezésének kérdését. Arra kerestem a választ, hogy egy ideális részvénypiaci modellnek milyen tulajdonságokkal kell rendelkeznie. Az elsődleges szempont az volt, hogy a modell képes legyen reprodukálni a piacon megfigyelt volatilitásmosolyt. További szempont volt, hogy a kiválasztott modell rendelkezzen a részvénypiacok stilizált tulajdonságaival mint például az áttételi hatás, vagy a vastag szélűség. Két kategóriából soroltam fel modelleket. A determinisztikus volatilitásmodellek közül lényeges volt az időfüggő volatilitású Black-Scholes modell, és a lokális volatilitás modell. A sztochasztikus volatilitás modellek közül említettem a diffúziós, az ugró-diffúziós és a tiszta ugró modelleket. Lényeges szempont a modellválasztásnál, hogy mik azok a faktorok amik befolyásolják a termék árát. Egyes termékek mint például a barrier opció, érzékenyek a volatilitás trajektóriájára.

Ezen termékek árazásához a volatilitás teljes trajektóriáját modellezni kell, amire egy sztochasztikus volatilitás modell alkalmas. Más termékek, mint például a bináris opció vagy a hagyományos call opció, nem függenek expliciten a volatilitás trajektóriájától, ezek árazására megfelelő lehet egy determinisztikus volatilitás modell is. Mivel a sávós hozamfelhalmozó előállítható bináris opciók összegeként, ezért nem érzékeny a sztochasztikus volatilitásra. Azonban ezeket a termékeket ritkán árusítják önmagukban, általában további egzotikus tulajdonságú kifizetésekkel társítják őket. Emiatt az elemzés további részéhez választottam mindkét modellkategóriából egyet: a determinisztikus modellek közül az időfüggő volatilitású Black-Scholes modellt, a sztochasztikus modellek közül pedig a Heston modellt.

A továbbiakban ezt a két modellt mutatom be részletesebben. Ismertetem a formulákat a call opcióra és a bináris opcióra mindkét esetben. A Heston modell esetén nem teljesen zárt a formula, mivel egy integrál alakjában adható meg, azonban ez az integrál jól közelíthető numerikus módszerek segítségével. Végül a Heston modell szimulációját is részletezem, arra az esetre ha egy előbb említett egzotikus verzióját akarnánk árazni a terméknek.

A szakdolgozat utolsó részében az R programnyelvben implementálom az előbbi fejezetekben ismertetett két modellt. A modelleket az S&P500 indexre kiírt call opciókra három lejáratra kalibrálom. A kalibrálás után az mondható el, hogy a Heston modell sokkal jobban illeszkedik a piaci adatokra, mint az időfüggő volatilitású Black-Scholes modell. Ezt az magyarázza, hogy az időfüggő Black-Scholes modell nem tudja lekövetni az ár változását a kötési árfolyam dimenziójában, míg a Heston modell igen. Ezután érzékenységvizsgálatot végzek a termék paramétereire és a Heston modell paramétereire. A termék paramétereinek közül a lejárat növelésével nő a termék ára is, hiszen egyre távolabb kerülnek a kupongyűjtési időpontok, így kisebb eséllyel esik bele ebbe a részvényárfolyam, továbbá a diszkontálás hatása is erősebb. A sáv szélességének növelésével - a vártnak megfelelően - a termék ára nő.

A Heston modell paramétereinek vizsgálatánál arra voltam kíváncsi, hogy a sávós hozamfelhalmozó ugyanúgy reagál-e a paraméterváltozásokra, mint a hagyományos call opció. Az érzékenységvizsgálat eredményeképp az mondható el, hogy nem viselkedik ugyanúgy a két termék. A sávós hozamfelhalmozónál a sáv helye nagyban befolyásolja azt, hogy miképp függ az ár, a Heston modell paramétereitől. Ebből arra a következtetésre jutottam, hogy nem optimális megoldás az, ha a Heston modellt a piacon megfigyelt call opciók árait kalibráljuk. Ugyanis a nagy eltérés miatt azok a paraméterek amiket call opciókra optimalizáltunk, egyáltalán nem biztos, hogy a hozamfelhalmozó esetén is optimálisan illeszkednek. Ideális esetben a piacon megfigyelt sávós hozamfelhalmozó árakra kellene kalibrálni a modellt, azonban ilyen adat csak nagyobb cégeknek áll rendelkezésre.

A szakdolgozatban bemutattam a sávós hozamfelhalmozó árazását két piaci modellben, kitérve a modellek kalibrálására is. Egy esetleges jövőbeli kutatás témája lehetne más piaci

modellek vizsgálata, vagy a sávos hozamfelhalmozó egzotikus verzióinak elemzése.

Szószedet

- **calibration:** kalibráció - az a folyamat amikor a modell paramétereit piaci adatokra illesztik.
- **deterministic volatility model:** determinisztikus volatilitás modell - olyan modell amelyben a volatilitás determinisztikus függvénye más faktoroknak.
- **digital option:** digitális/bináris opció - olyan opció ami egységnyi kifizetést biztosít ha az alaptermék meghaladja a kötési árfolyamot
- **equity-linked derivative:** részvényhez kötött derivatíva
- **implied volatility:** implikált volatilitás
- **jump-diffusion:** ugró diffúzió - olyan modell amelyben a diffúziós tagon kívül egy véges aktivitású ugrófolyamat is befolyásolja az árfolyamdinamikát
- **leverage effect:** áttételi hatás - mely szerint a hozamok negatívan korrelálnak a volatilitással
- **local volatility model:** lokális volatilitás modell
- **market model:** piacmodell - olyan matematikai modell amelyet valamilyen piac leírására használunk
- **mean-reverting proces:** átlaghoz visszahúzó folyamat
- **observation period:** megfigyelési időszak - az a periódus amiben megfigyelik hogy a range accrual termék a sávon belül tartózkodik-e
- **over the counter:** tőzsdén kívüli - olyan derivatívákra használjuk amiket tőzsdén kereskednek
- **payoff:** kifizetés - a derivatíva kifizetésfüggvénye
- **range accrual:** sávós hozamfelhalmozó - exotikus derivatíva ami kuponokat halmoz fel ha az alaptermék egy meghatározott sávban van. A kuponokat a periódus végén fizeti ki.
- **risk-neutral measure:** kockázatsemleges mérték
- **risk-free rate:** kockázatmentes kamatláb
- **spot price:** azonnali árfolyam

- **stochastic volatility model:** sztochasztikus volatilitás modell - olyan modell amiben a volatilitás időben sztochasztikusan változik
- **strike:** kötési árfolyam
- **structured product:** strukturált termék - hagyományos termékeknek a strukturált kombinációja. Pl. hagyományos kötvény részvényhez kötött kuponfizetéssel.
- **time-dependent:** időfüggő
- **underlier:** alaptermék
- **vanilla call option:** call opció - vételi jogot biztosító opció
- **volatility smile:** volatilitás mosoly - a volatilitás ábrázolása a kötési árfolyam függvényében